8-1-1982

Design Optimization of Slider-Crank Mechanisms Subject to Coulomb Bearing Friction

Anthony J. Pascuzzi

DESIGN OPTIMIZATION OF SLIDER-CRANK MECHANISMS SUBJECT TO COULOMB BEARING FRICTION

by

Anthony J. Pascuzzi

Bachelor of Science, Mechanical Engineering, 1979

Bachelor of Science, Electrical Engineering, 1980

A Thesis

Submitted to the Graduate Faculty

of the

University of North Dakota

in partial fulfillment of the requirements

for the degree of

Master of Science

Grand Forks, North Dakota

August, 1982

This thesis submitted by Anthony J. Pascuzzi in partial fulfillment of the requirements for the Degree of Master of Science from the University of North Dakota is hereby approved by the Faculty Advisory Committee under whom the work has been done.

J. Peter Sadler
(Chairman)

Ed Adam

D P Nairnith

This thesis meets the standards for appearance and conforms to the style and format requirements of the Graduate School of the University of North Dakota, and is hereby approved.

Dean of the Graduate School

Permission

Title DESIGN OPTIMIZATION OF SLIDER-CRANK MECHANISMS SUBJECT TO COULOMB BEARING FRICTION

Department Mechanical Engineering

Degree Master of Science

In presenting this thesis in partial fulfillment of the requirements for a graduate degree from the University of North Dakota, I agree that the Library of this University shall make it freely available for inspection. I further agree that permission for extensive copying for scholarly purposes may be granted by the professor who supervised the thesis work or, in his absence, by the Chairman of the Department or the Dean of the Graduate School. It is understood that any copying or publication or other use of this thesis or part thereof for financial gain shall not be allowed without my written permission. It is also understood that due recognition shall be given to me and to the University of North Dakota in any scholarly use which may be made of any material in my thesis.

Signature _____

Date _____

TABLE OF CONTENTS

TABLE OF CONTENTS, Continued

LIST OF FIGURES

LIST OF FIGURES, Continued

LIST OF TABLES

ACKNOWLEDGMENTS

The author wishes to express sincere appreciation to Dr. J.P. Sadler, Dr. D.P. Naismith, and Dr. E.L. Adams for serving as members on the Faculty Advisory Committee.

Additional thanks are extended to the clerical and drafting staff of the Engineering Experiment Station for their roles in preparing the rough and final drafts of the thesis.

ABSTRACT

Optimization techniques are applied to the design of slider-crank mechanisms operating as single acting compressors subject to Coulomb bearing friction. The dynamic force analysis is performed by the solution of a set of nonlinear equations in dimensionless form. The optimization results presented are for various cases of inertia, friction, and external loading.

The optimization procedure developed minimizes a weighted sum of the input work and bearing shear stress by adjusting the mechanism's dimensions. The independent dimensions that are varied are the connecting rod length, the offset, and the three bearing radii. The results of the optimization are different optimum slider-crank linkage configurations, where each linkage minimizes a different level of the work-stress combination.

This optimization procedure can be useful in the design of slider-crank mechanisms employed in compressors. Further, the method can be expanded to other mechanism types and loading forms.

NOMENCLATURE

A_p	Surface area of the piston face
A_{x3}	Linear acceleration of the connecting rod center of mass in the x direction
A_{y3}	Linear acceleration of the connecting rod center of mass in the y direction
A_{41}	Linear acceleration of the slider with respect to the frame
d	Connecting rod diameter
E	Young's modulus
F_{ij}	Force member i exerts upon member j
F_L	External force applied to the slider
F_M	Maximum reaction forces
F_{xij}	Force member i exerts upon member j in the x direction
F_{yij}	Force member i exerts upon member j in the y direction
H	Offset of the slider
I	Inertia of member i about it's center of mass
k	Specific heat ratio
L	Length of the journal bearing
M_i	Mass of member i

P Pressure

P_a Ambient pressure

P_e Exhaust pressure

P_i Inlet pressure

R_F Radius of the friction circle

R_i Radius of bearing i

R_{LX} Distance from pin 2 to the center of mass of the connecting rod

R_{L2} Crank length

R_{L3} Connecting rod length

S Stroke

T_{ij} Torque exerted by member i on member j

T_{in} Input torque

V_{41} Linear velocity of the slider with respect to the frame

W Input work

w Weighting factor

α Bearing clearance

α_i Angular acceleration of member i

β Material independent shear stress, the stress factor

γ Clearance volume ratio

θ_i Angular position of member i

μ Coefficient of friction

μ_p Poisson's ratio

ρ Mass density

τ Shear stress

ω_i Angular velocity of member i

CHAPTER 1

INTRODUCTION

To date, a number of mechanism optimization studies have been conducted; however, these studies have neglected dry or Coulomb friction effects in mechanisms. Coulomb friction is the resistance encountered when two contacting surfaces slide over each other in the absence of any fluids or films [1]. A survey of the existing mechanical optimization literature found studies dealing with mechanism balancing, position synthesis, and stress minimization, to name a few of the topics [2,3,4,5,6,7].

This study performs a mechanism optimization considering the effects of friction on mechanism behavior. When optimizing a mechanism, the design parameters of the mechanism are adjusted until the minimum value of an objective function is obtained. The objective function in this investigation is a combination of the stresses generated in the mechanism members and the work required to drive the mechanism. The major variables used to calculate the work and stresses are the forces in the mechanism. These forces are a function of mechanism geometry, coulomb friction, inertia effects, and the applied load.

The objective of this thesis is to develop a procedure to determine the optimum configuration of a slider-crank mechanism that simultaneously minimizes the stresses generated and the input work for a given magnitude of coulomb friction. If it proves impossible to produce the simultaneous minimization, a family of mechanism configurations will be developed in which every configuration corresponds to a different level of minimization in the work-stress combination. All members of this mechanism family are

subjected to the same external load, the same magnitude of friction effects, and are driven at the same speed. The particular application used as an example in this study is the slider-crank linkage loaded as a single-acting compressor.

1-1 Model of Coulomb Friction

Despite extensive study, a complete explanation of the mechanism of Coulomb friction does not as yet exist [8,9,10]. What is known is that the effect of coulomb friction is a resistance to the relative motion of the contacting surfaces. The resistance is modeled as a force that is referred to as the friction force. The conditions that are usually applied when modeling the friction force are stated as follows:

1. The friction force is directly proportional to the normal force pressing the surfaces together.
2. The friction force is independent of the contacting area of the two surfaces.
3. The magnitude of the friction force is independent of the relative velocity between the surfaces.
4. The proportionality constant relating the friction force to the normal force is dependent upon the nature of the contacting surfaces [8].

Studies are in progress [9] that use a model of the friction force magnitude that is velocity dependent for small relative velocities. For large relative velocities, the friction force is, as stated above, essentially independent of variations in the relative velocity. In this analysis, the classical friction force model, employing characteristics (1) through (4) from above, is used. Note that when the relative velocity between the contacting surfaces is zero, the friction force is also zero since the friction force is the resistance encountered when two contacting surfaces slide over each other or have a nonzero relative velocity. The model of

the friction force is then:

$$F_f = -\mu|F_n|\text{sgn}(v) \tag{1-1}$$

where F_f is the friction force, F_n is the normal force, μ is the coefficient of friction, and v is the relative velocity of the contacting surfaces. The signum function, sgn(v), is defined as:

$$\text{sgn}(v) = \frac{|v|}{v} = \begin{cases} 1 \text{ for } v > 0 \\ 0 \text{ for } v = 0 \\ -1 \text{ for } v < 0 \end{cases} \tag{1-2}$$

When the relative velocity switches directions, the direction of the friction force is reversed, and when the relative velocity is zero, the signum function is zero, and therefore, the force is zero.

1-2 Mechanism Description

The mechanism being optimized is a planar slider crank linkage. The mechanism, as shown in Figure 1-1, consists of four links, three pins, and one translational sliding contact. The links are the frame (link 1), crank (link 2), connecting rod (link 3), and the slider (link 4). The frame is assumed to be stationary and the links have relative motion to the frame. The length, mass, inertia, positions, motions, reaction forces, and reaction torques for each link are subscripted by the link number associated with the link.

There are four connections between the links. Three of these are pin connections and the other is a translational sliding contact. The pin connections, also referred to as journal bearings (Figure 1-2), allow a relative motion between the contacting members which is rotation about one axis. The pin connections occur between the frame and crank, the crank

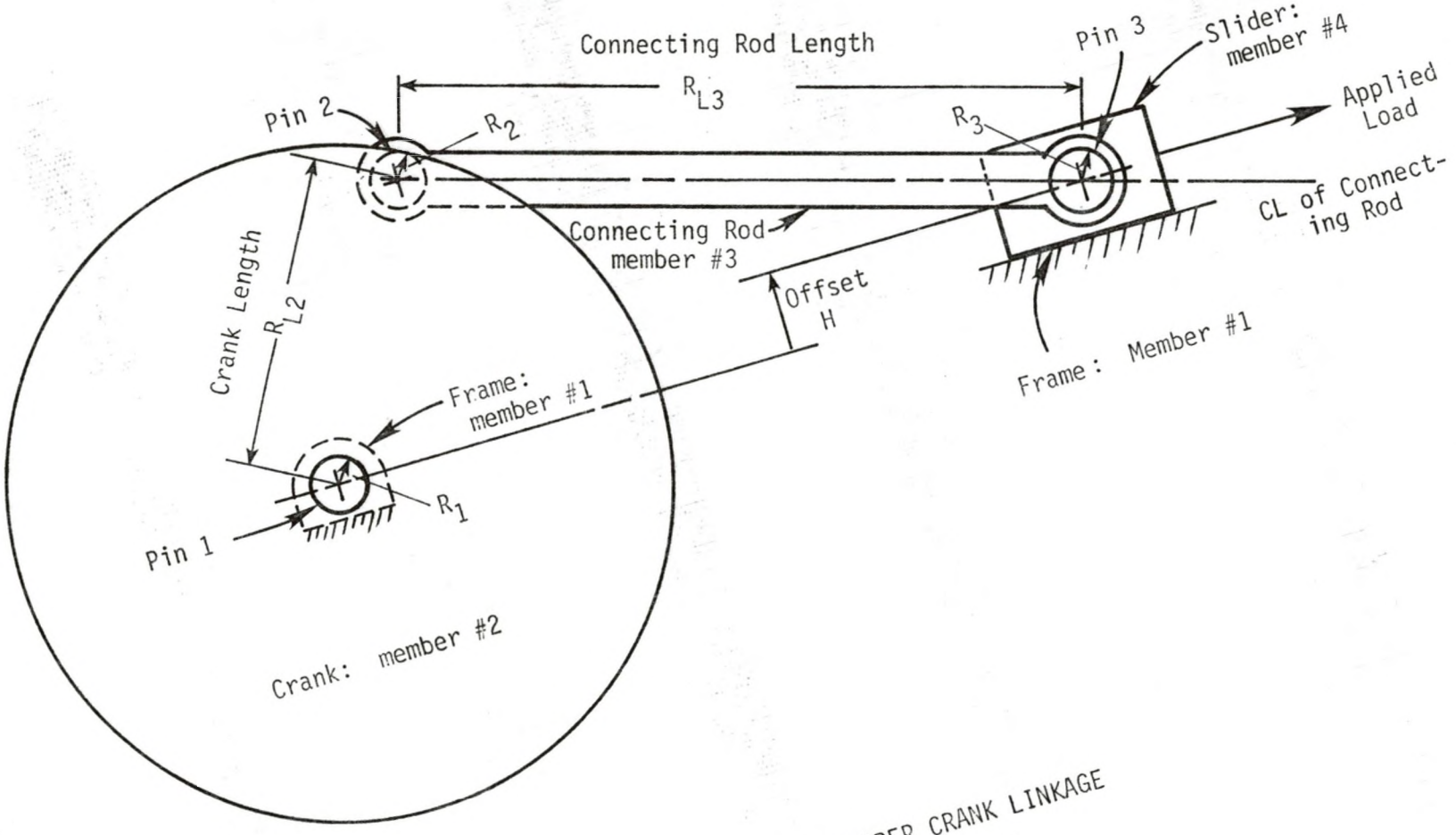

FIGURE 1-1 - SLIDER CRANK LINKAGE

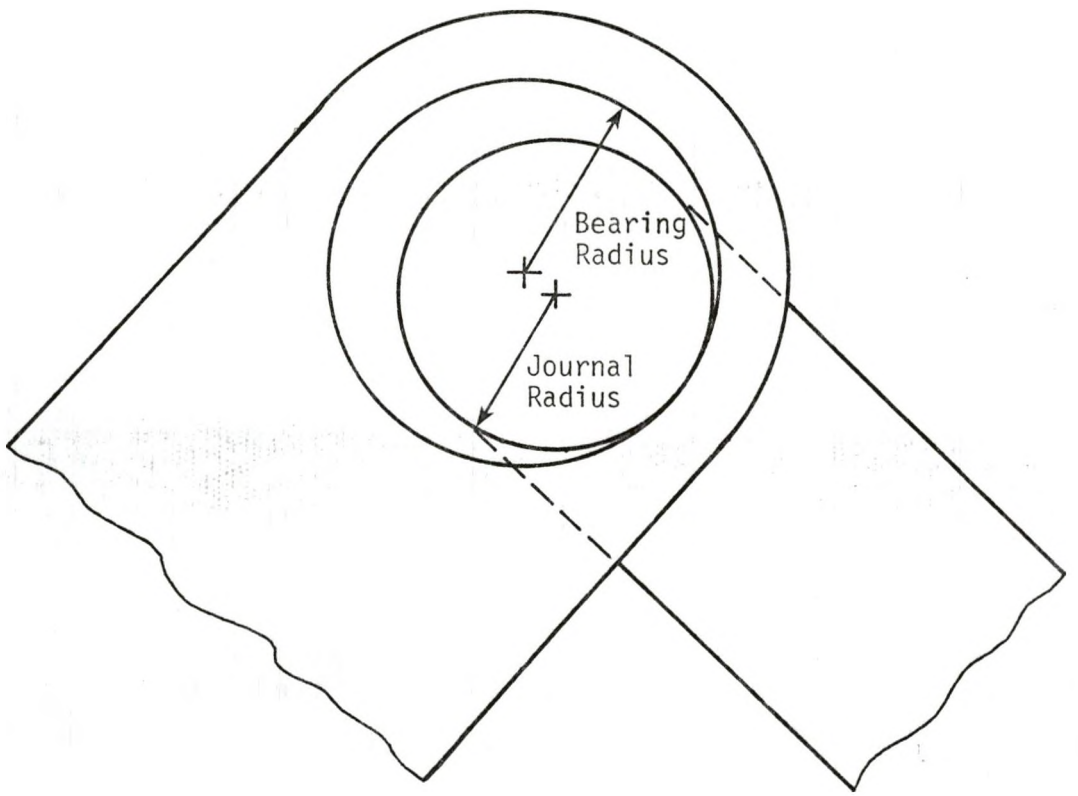

FIGURE 1-2 - JOURNAL BEARING

and connecting rod, and between the connecting rod and slider. These connections are referred to by pin numbers one, two, and three, respectively. The fourth connection is a sliding contact which allows a relative motion of translation in one of the axial directions. This connection occurs between the slider and the frame. The mechanism is planar; that is, all of its positions, motions, and forces are represented in two dimensions.

1-3 Optimization Description

The specific design criteria of the mechanism are the minimization of the required input work and the possible simultaneous minimization of stresses in the mechanism. The input work is applied to the crank and is the energy required to drive the mechanism through a complete cycle. The work is required to offset the effects of friction and inertia, and also to drive the piston through a complete compression cycle. The input work reflects the operating cost of the mechanism, and is determined by integrating the product of the external torque applied to the crank and the crank velocity over the time for a complete cycle of the crank.

The stress of particular interest is the shear stress in the journal bearings. This shear stress is the result of the distortions in the contacting surfaces of the journal bearings produced by the forces transmitted through the bearings. The belief is that a crack originates a small distance into the surface, at the location of the maximum shear stress, and then progresses to the surface. When the crack reaches the surface, a fatigue failure occurs [11]. The larger the shear stress is, the sooner the surface will fail. The shear stress can then be used to represent, in an inverse fashion, the mechanism life.

The magnitude of the shear stress is calculated by using the Hertz equations for contacting cylinders [11]. Figure 1-3 shows internally contacting cylinders pressed together by a normal force, F_N. The region of distortion has a width 2b and an elliptical pressure distribution across this width. The half-width of the area of contact is given by

$$b = \sqrt{\frac{2F_N}{\pi L} \frac{[(1 - \mu^2_{P1})/E_1 + (1 - \mu^2_{P2})/E_2]}{(1/d_1) - (1/d_2)}} \qquad (1\text{-}3)$$

where F_N is the instantaneous force normal to the contacting area pressing the cylinders together, L is the cylinder length, d_1 is the inner cylinder diameter, d_2 is the outer cylinder diameter, E_i is the modulus of elasticity for each cylinder, and μ_{Pi} is the value of Poisson's ratio for each cylinder. The inner cylinder is the journal while the outer cylinder is the bearing. The maximum pressure is then

$$P_{max} = \frac{2 \ F_N}{\pi \ b \ L} \qquad (1\text{-}4)$$

The largest value obtained by the maximum shear stress is three-tenths of the maximum pressure, P_{max}, and occurs at a distance b below the surface [11].

Assuming that the journal the bearing are made of the same material, the equation for the maximum shear stress is written as

$$\tau_{max} = 0.3\sqrt{\frac{F_M}{L \ R} \frac{E \ \alpha}{2\pi(1 - \mu_p^2)(1 + \alpha)(1 + \mu^2)^{1/2}}} \qquad (1\text{-}5)$$

where F_M is the maximum transmitted force, μ is the coefficient of friction, R is the journal radius, and α is the percent difference between journal and bearing diameters. For most mechanisms, α is usually less than 0.2

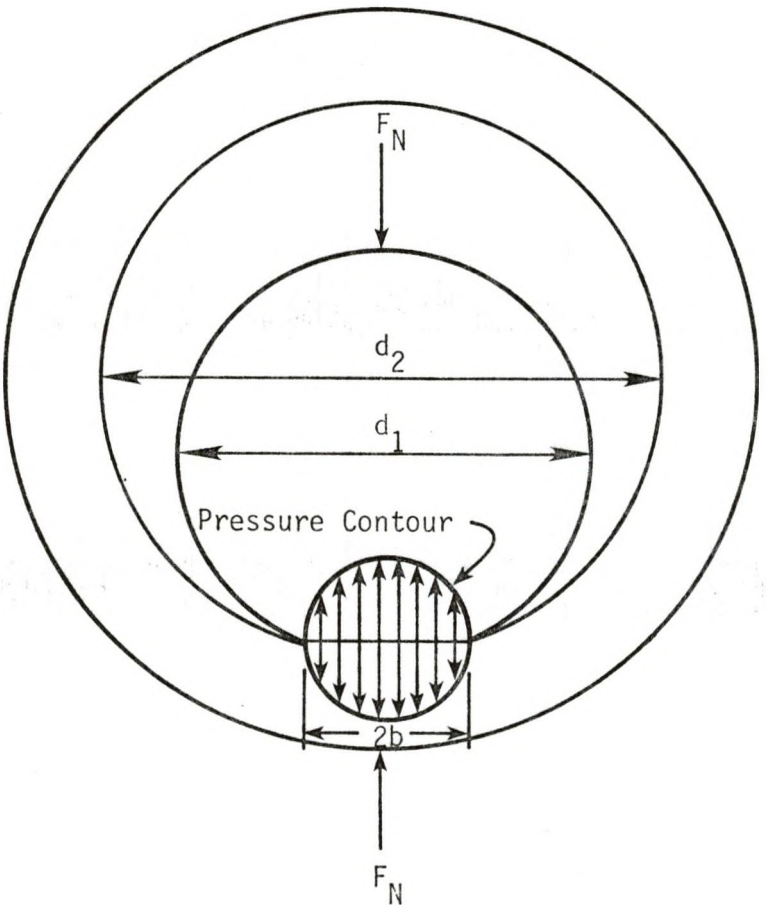

FIGURE 1-3 - HERTZ STRESS DISTRIBUTION BETWEEN INTERNALLY CONTACTING CYLINDERS

percent and is defined as [10]:

$$\alpha = \frac{d_2 - d_1}{d_2} \tag{1-6}$$

The factor $F_M/(1 + \mu^2)^{1/2}$ is the component of the maximum transmitted force in the direction normal to the surface. The maximum transmitted force is important since the largest shear stress in a particular bearing is produced by the largest transmitted force in that bearing.

CHAPTER 2

APPLICATION TO A SINGLE ACTING COMPRESSOR

As stated in Chapter 1, the mechanism to be optimized is the slider crank linkage loaded as a compressor. The optimum mechanism is that with design parameter values which minimize the objective function subject to mechanism constraints. To facilitate the optimization process, the mechanism analysis is dimensionless.

2-1 Mechanism Constraints and Design Parameters

Constraints are placed upon the mechanism geometry, motion, and loading to provide a common basis for comparing the performance of different configurations. The first group deals with the loading, and are:

1. The load is based on an ideal single-acting compressor.
2. The maximum and minimum pressures in the cycle are constant.
3. The working fluid is an ideal gas.
4. The work required to complete the ideal compression process is constant and independent of the mechanism configurations.
5. The clearance volume is a fraction γ of the displaced volume swept by the piston displacement.

The second group of constraints deal with the mechanism's motion and are as follows:

6. For any mechanism selected, the crank must be able to make a complete revolution.
7. The mechanism's stroke is constant (maximum piston displacement).
8. The crank rotates at a constant angular velocity.

The third and final group of constraints deal with the mechanism's geometry and they are:

9. The crank is a uniform disk rotating about its center of mass.

10. The connecting rod is a uniform rod with a length to diameter ratio of ten, and has bearing housings attached to its ends.

11. The slider's mass and surface area are constant.

12. The length of the journal bearing is equal to the connecting rod diameter.

13. The clearance between the journal and bearing is a tenth of a percent of the journal diameter.

14. The mechanism is made entirely of one material.

The available design parameters are reduced when constraints 6 and 7 are applied. If the connecting rod length, R_{L3}, and the offset, H, are assumed to be known then the crank length, R_{L2}, can be calculated. The link lengths are all measured as the distance between the centers of the journal-bearings attached to that link. Figure 2-1 shows the extremes of the slider positions for an assumed offset and connecting rod length with a constant stroke, S. The terms X_1 and X_2 are respectively the minimum and maximum slider positions and their difference is the stroke. A careful examination of Figure 2-1 reveals the following relationships:

$$X_1 = ((R_{L3} - R_{L2})^2 - H^2)^{1/2} \qquad (2\text{-}1)$$

$$X_2 = ((R_{L3} + R_{L2})^2 - H^2)^{1/2} \qquad (2\text{-}2)$$

Taking the difference between eq. (2-2) and eq. (2-1) and simplifying results in:

$$R_{L2} = [(4S^2R_{L3}^2 - S^4 - 4S^2H^2)/(16R_{L3}^2 - 4S^2)]^{1/2} \qquad (2\text{-}3)$$

so the crank length is a function of the stroke, offset, and connecting rod length. Therefore, the design parameters in this optimization process are:

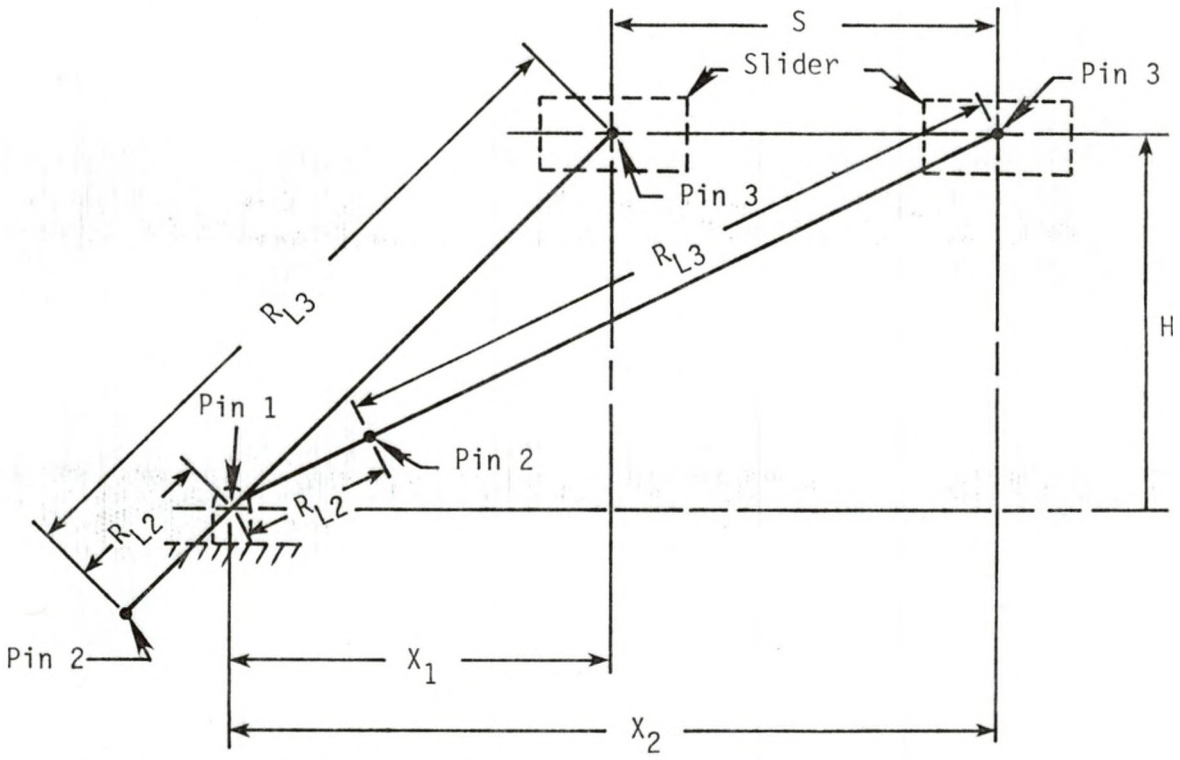

FIGURE 2-1 - EXTREMES OF THE SLIDER POSITIONS

1. The three bearing diameters
2. The connecting rod length
3. The slider offset

2-2 Model of the Mechanism Loading Function

It has been frequently stated that the mechanism is to be loaded as a single-acting compressor. In a single-acting compressor the working fluid is compressed between the cylinder walls and one side of the piston, as shown in Figure 2-2. The terms piston and cylinder wall are synonymous to the slider and frame, respectively, and are used interchangeably throughout this thesis. A typical pressure-volume (P-V) diagram for a compression cycle is shown in Figure 2-3. The components of the cycle are: compression of the working fluid from points 1 to 2, exhaust from 2 to 3, expansion from 3 to 4, and intake from 4 to 1. The irregularities in the curves representing the exhaust and intake portions of the cycle are due to the valve action. The working fluid is being exhausted into a reservoir at a pressure P_e, and is being drawn into the cylinder from a reservoir at a pressure of P_i or the intake pressure. The other side of the piston is exposed to a pressure P_a, or the ambient pressure. The volume V_M is the maximum volume enclosed by the cylinder walls and piston while V_C, the clearance volume, is the minimum value of the enclosed volume. The clearance volume is always greater than zero.

When modeling the compression cycle, some assumptions need to be made. These assumptions were stated as the constraints in the previous section. These constraints will now be elaborated upon and expanded. First, the working fluid is an ideal gas with a specific heat ratio, k, of 1.4. Secondly, the compression cycle is assumed to be ideal, therefore, the intake and exhaust portions of the cycle are isobaric, and the compression and

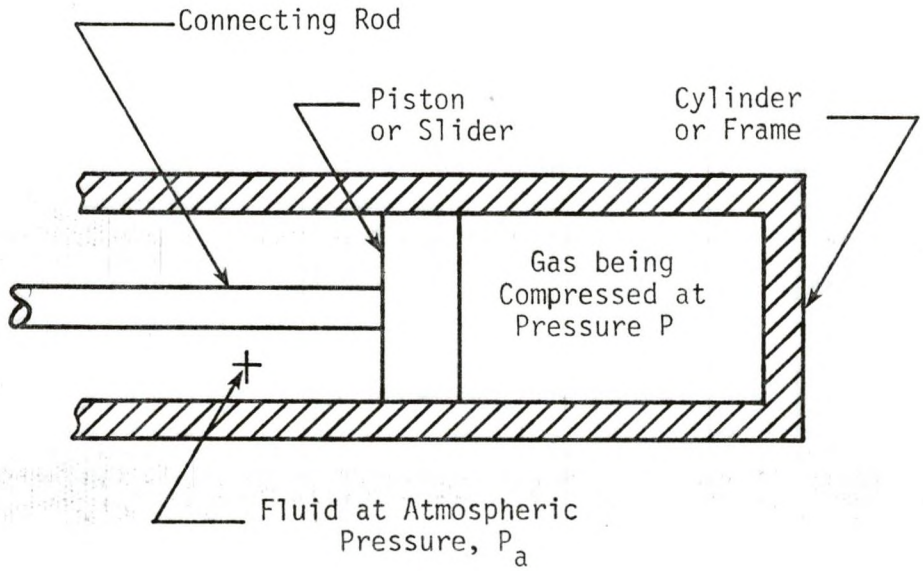

FIGURE 2-2 - SECTIONED VIEW OF PISTON AND CYLINDER

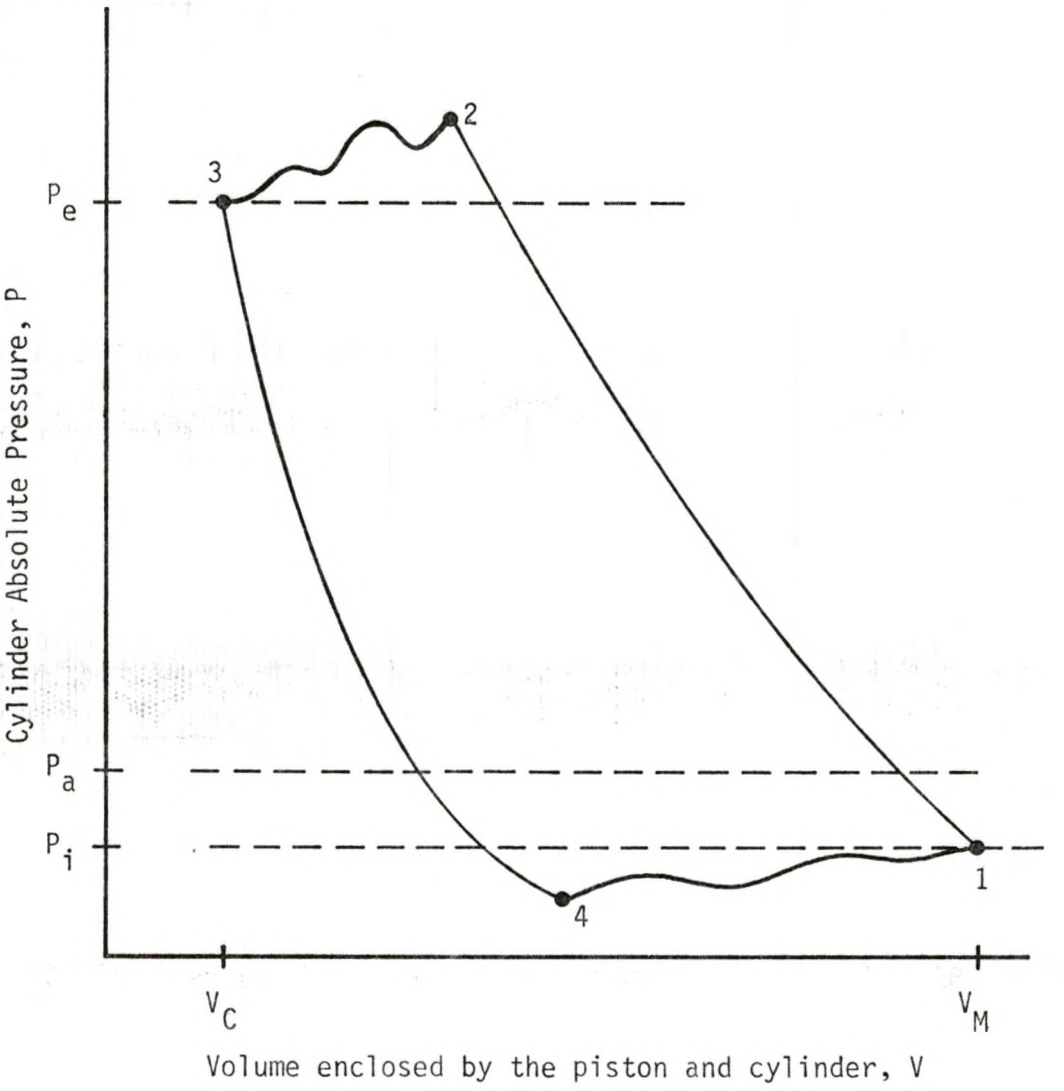

FIGURE 2-3 - TYPICAL PRESSURE-VOLUME DIAGRAM FOR A SINGLE ACTING COMPRESSOR

expansion portions of the cycle are isentropic [12]. The volume enclosed by the cylinder for a specific displacement of the piston V is

$$V = V_D + V_C \tag{2-4}$$

where V_C is the clearance volume, and V_D is the volume swept by the piston displacement. The volume V_D, can vary from zero to $V_M - V_C$, and can be determined as a function of the piston displacement.

$$V_D = \frac{D}{S}(V_M - V_C) \tag{2-5}$$

where D represents the piston displacement as shown in Figure 2-4, and S is the stroke. The clearance volume is a fraction, γ, of the displacement volume, therefore,

$$V_C = (V_M - V_C) = (S)(A_p)\gamma \tag{2-6}$$

where A_p is the surface area of the piston. Eq. (2-4) is then written as

$$V = (\frac{D}{S} + \gamma)(S)(A_p) \tag{2-7}$$

Noting the relationships for an isobaric process, the pressure is constant as a function of the volume, and second for an isentropic process

$$PV^k = \text{Constant} \tag{2-8}$$

Then Figure 2-4 can be constructed. Figure 2-4 is used to model the absolute cylinder pressure. The equations used in this model are, for the exhaust portion of the cycle

$$P = P_e \tag{2-9}$$

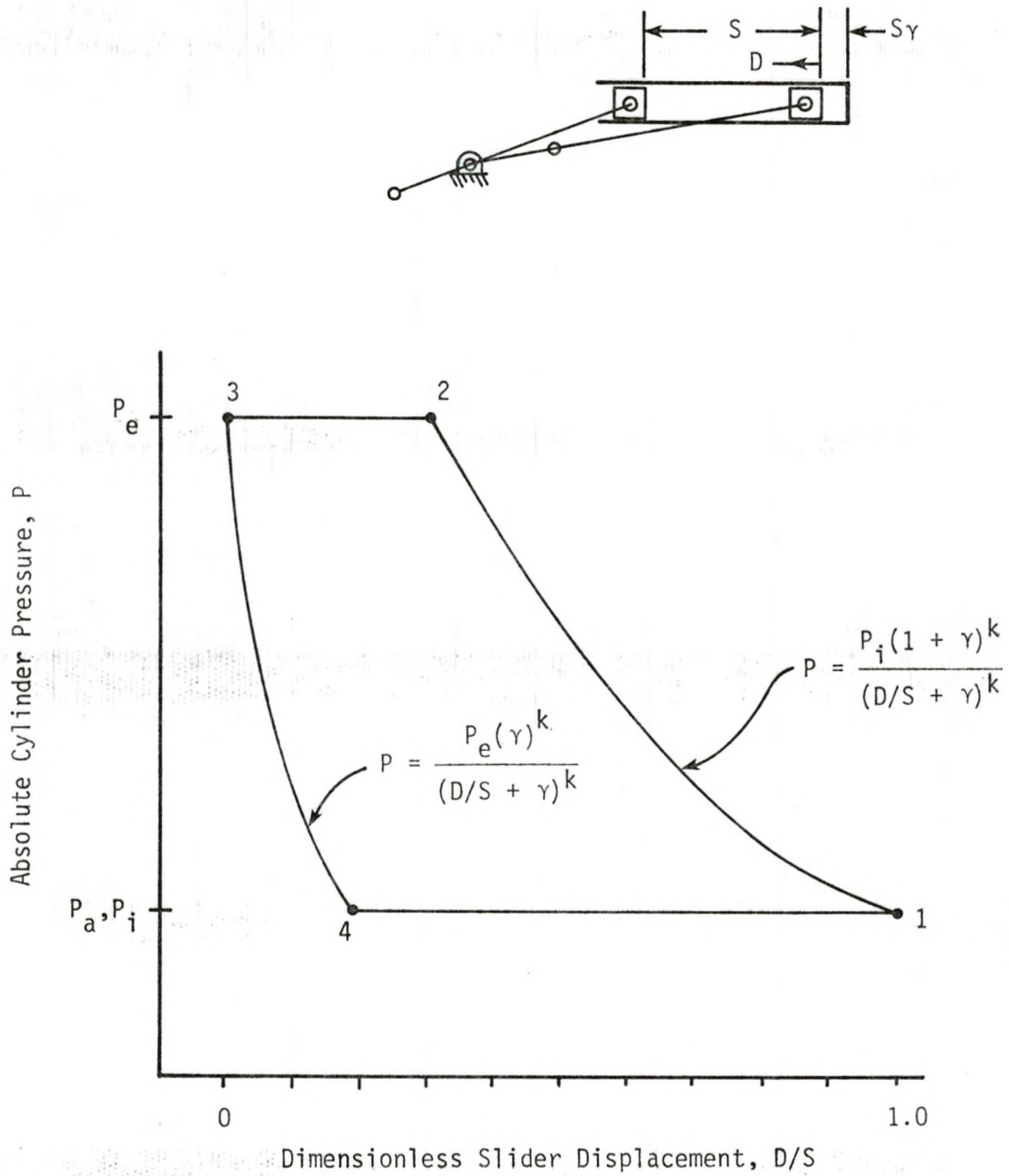

FIGURE 2-4 - MODEL OF THE COMPRESSION CYCLE

For the expansion portion of the cycle,

$$P = \frac{P_e(\gamma)^k}{(D/S + \gamma)^k} \tag{2-10}$$

For the intake portion of the cycle,

$$P = P_i \tag{2-11}$$

For the compression portion of the cycle,

$$P = \frac{P_i(1 + \gamma)^k}{(D/S + \gamma)^k} \tag{2-12}$$

where k is the specific heat ratio and equals 1.4. The different portions of the cycle intersects at points 1, 2, 3, 4, and the slider's positions of D_1 and D_3 are simply the maximum and minimum slider displacements. The values of D_2 and D_4 can be determined to be

$$D_4 = \left[\left(\frac{P_e}{P_i}\right)^{1/k} \gamma - \gamma \right] S \tag{2-13}$$

$$D_2 = \left[\left(\frac{P_i}{P_e}\right)^{1/k} (1 + \gamma) - \gamma \right] S \tag{2-14}$$

The load applied to the slider assuming the open face is exposed to the ambient pressure and the connection between the slider and connecting rod has negligible area is

$$F_L = -(P - P_a)A_p \tag{2-15}$$

2-3 Dimensional Analysis

The only way to completely analyze the design parameters of the mechanism is to mathematically model the mechanism. To aid this analysis the mathematical model is made dimensionless. The dimensionless model has

three principle advantages: 1) it reduces the number of independent variables, 2) it makes it easier to present the data, and 3) it makes the information more useful because it has been generalized to pertain to a broader range of constraints and design parameters. The variables in this study are the crank velocity (ω_2), crank length (R_{L2}), connecting rod length (R_{L3}), the offset (H), the bearing radii (R_1, R_2, R_3), slider mass (M_4), stroke (S), density of the material (ρ), Young's modulus (E), Poisson's ratio (μ_p), piston face area (A_p), intake pressure (P_i), exhaust pressure (P_e), clearance volume ratio (γ), and the coefficient of friction (μ). In this dimensional analysis, the basic dimensions are length, time, and mass; these are characterized by the stroke, crank period ($1/\omega_2$) and the slider mass. The dimensionless lengths (i.e., $\bar{R}_1$, $\bar{R}_{L2}$, etc.) are fractions of the stroke. Buckingham showed that the number of independent dimensionless groups of variables needed to correlate the variables in a given process is equal to n-m, where n is the number of variables involved and m is the number of basic dimensions included in the variables [13]. Therefore, distance, area, and volume are made dimensionless by dividing by stroke, stroke squared, and stroke cubed, respectively. Time dimensions are removed by dividing by the period or by multiplying by the crank velocity (ω_2). Mass is made dimensionless by dividing by the slider's mass.

The first equation to be nondimensionalized is the equation for the crank length, eq. (2-3). The dimensionless crank length, $\bar{R}_{L2}$, is then

$$\bar{R}_{L2} = \frac{R_{L2}}{S} = \left(\frac{4\bar{R}_{L3}^{\,2} - 1 - 4\bar{H}^2}{16\,\bar{R}_{L3}^{\,2} - 4} \right) \qquad (2\text{-}16)$$

The load applied to the slider, eq. (2-15), in dimensionless form is

$$\overline{F}_L = -(\overline{P} - \overline{P}_a)\,\overline{A}_p \qquad (2\text{-}17)$$

Both of these equations help make the model more generalized because now all lengths are fractions of the stroke and secondly, while the dimensionless combinations $\overline{P}_a\,\overline{A}_p$ and $\overline{P}_e\,\overline{A}_p$ remain constant the individual pressures and area values may vary.

The objective function is some combination of the input work and the bearing shear stresses. Work which has units of $M\,L^2/T^2$ is simply made dimensionless by dividing by $M_4\,S^2\,\omega_2{}^2$. The shear stress, which has units of $M/L\,S^2$, is given in dimensionless form by

$$\overline{\tau}_{max} = 0.3\sqrt{\frac{\overline{F}_M}{\overline{L}\,\overline{R}}\,\frac{\overline{E}\,\alpha}{2\pi(1-\mu_p{}^2)(1+\alpha)(1+\mu^2)^{1/2}}} \qquad (2\text{-}18)$$

where the dimensionless variables are as follows: $\overline{\tau}$ is the shear stress, $\overline{F}_M$ is the maximum transmitted force, $\overline{L}$ is the bearing length, $\overline{R}$ is bearing radius, and $\overline{E}$ is Young's modulus. A material independent dimensionless stress factor $\overline{\beta}$ is defined as

$$\overline{\beta} = \sqrt{\frac{\overline{\tau}_{max}}{\frac{\overline{E}\,\alpha}{(1-\mu_p{}^2)(1+\alpha)}}} = 0.3\sqrt{\overline{F}_M/(\overline{L}\,\overline{R}\,(1+\mu^2)^{1/2}\,2\pi)} \qquad (2\text{-}19)$$

where $\overline{\beta}$ will be used in the objective function instead of $\overline{\tau}$ because of it's more generalized form. Throughout this thesis dimensionless quantities are designated by a bar above the term.

CHAPTER 3

ANALYTICAL MODEL

To optimize the mechanism, numerous mechanism configurations are analyzed until the minimum of the objective function is found. A large number of mechanisms may have to be analyzed before the minimum is found. Because of the large number of mechanism configurations, a physical model is not practicle, therefore, a mathematical model is used in conjunction with a digital computer. Still, because of the large number of configurations possible, it would take a large amount of time to just randomly analyze mechanisms to find a minimum. To reduce the number of mechanisms that need to be analyzed a patterned search is used. The pattern used in this research is part of an optimization package that was developed by Afimiwala and Mayne [14]. The specific technique used is a variable metric search that is also referred to as the Davidon-Fletcher-Powell method [15].

A mathematical model of the slider crank linkage will now be developed. This model is divided into the following categories:

1. Kinematic Model
2. Dynamic-Force Model
    a. Neglecting the journal and bearing masses
    b. Including the journal and bearing masses

The kinematic model relates the position, velocity, and acceleration of the driven members to the position, velocity, and acceleration of the driving member. In this analysis, the driven members are the piston and connecting rod while the driving member is the crank. The frame is assumed to be

stationary and all measurements of position, velocity, and acceleration are made with it as the reference. All reaction forces and torques are obtained from the dynamic-force model in conjunction with the kinematic model as a function of the crank position. This analysis is referred to as a dynamic-force analysis because it includes the effects of all applied forces, torques, and inertia effects for each link [16].

3-1 Kinematic Model

To facilitate the kinematic analysis, the mechanism is redrawn in a skeleton form (Figure 3-1). When drawn in skeleton form, the links are dimensioned so that only those dimensions which affect their motion are considered. Figure 3-1 shows the positive orientations of all the variables. All linear quantities are positive if they are orientated to the right or top of the page. The rotational quantities are positive if they act in a counter-clockwise direction. The additional linear quantities are $\overline{V}_{41}$ and $\overline{A}_{41}$, the respective dimensionless velocity and acceleration of the piston, while $\overline{\omega}_i$ and $\overline{\alpha}_i$ are the respective dimensionless angular velocity and acceleration of link "i".

The solution of the kinematic analysis of a slider crank linkage can be found in most introductory machine design texts. The usual method used to obtain the solution is first to define the linkage in a complex coordinate system as shown in Figure 3-2. In this figure, the linkage is represented by complex polar vectors. The sum of these vectors define a closed path, a loop closure equation, therefore,

$$\overline{R}_{L2}e^{i\theta_2} + \overline{R}_{L3}e^{i\theta_3} = \overline{X}e^{io} + \overline{H}e^{i\pi/2} \qquad (3\text{-}1)$$

Equation (3-1) is then separated into its real and imaginary component to obtain the following

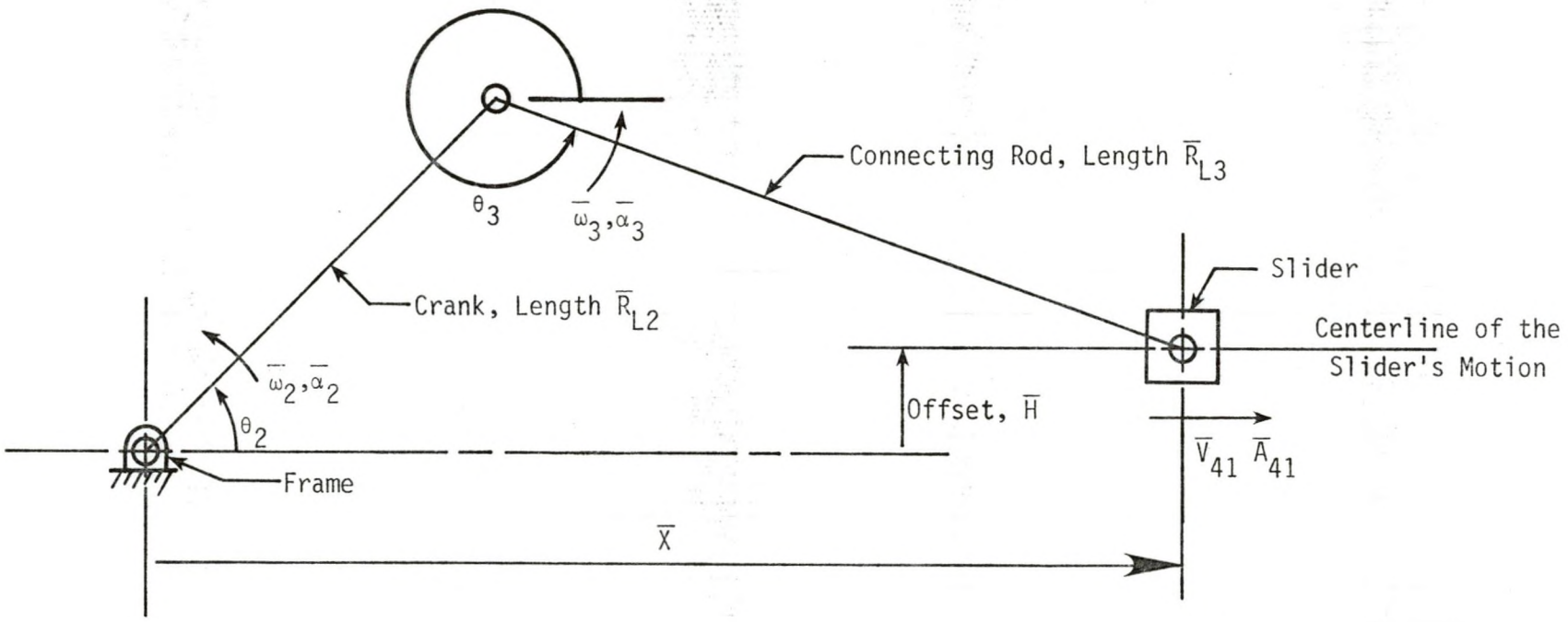

FIGURE 3-1 - SLIDER CRANK LINKAGE IN SKELETON FORM

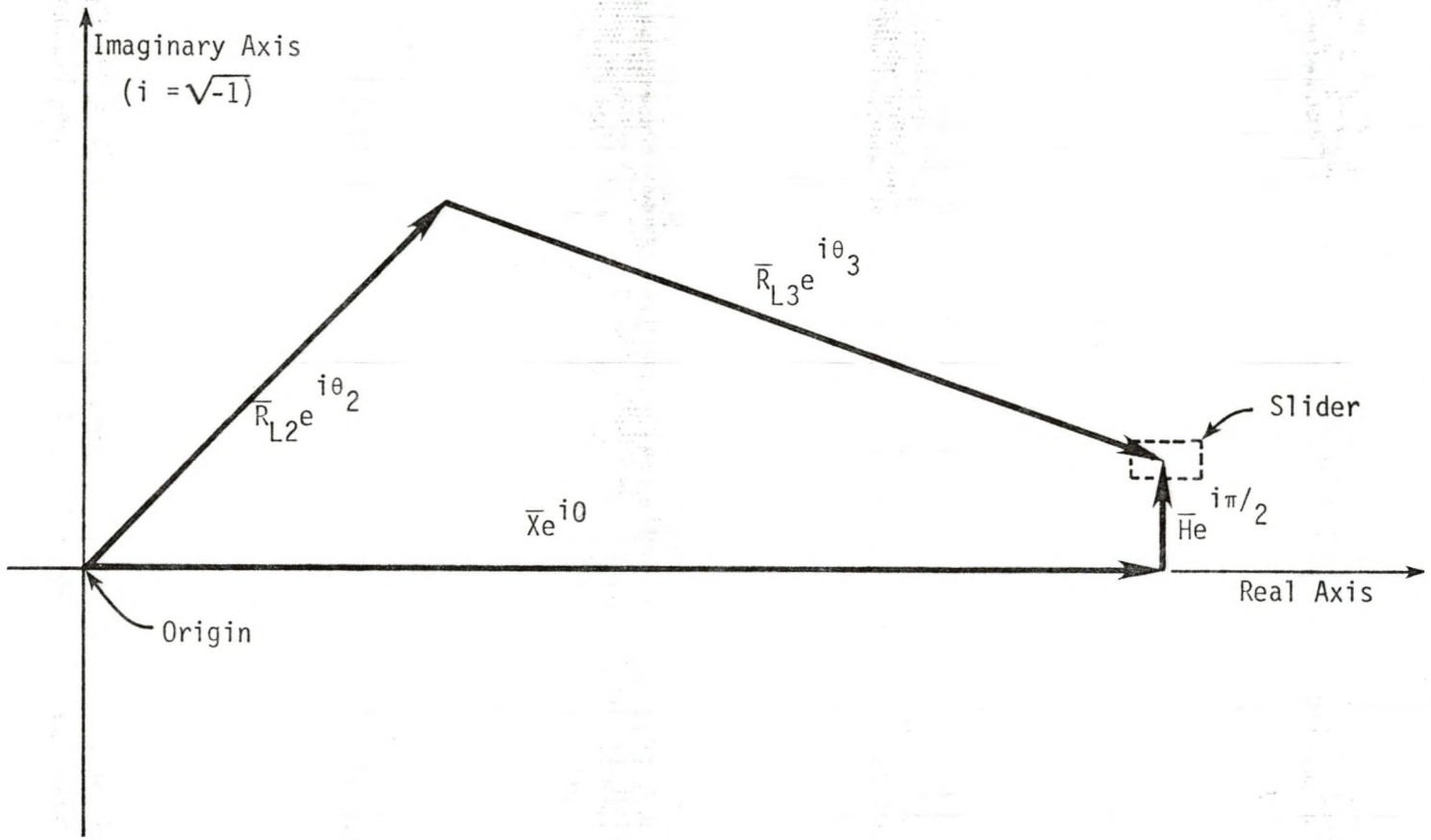

FIGURE 3-2 - LINKAGE IN A COMPLEX COORDINATE SYSTEM

$$\theta_3 = \arcsin\left(\frac{\bar{H} - \bar{R}_{L2}\sin\theta_2}{\bar{R}_{L3}}\right) \tag{3-2}$$

$$\bar{X} = \bar{R}_{L2}\cos\theta_2 + \bar{R}_{L3}\cos\theta_3 \tag{3-3}$$

The velocities are obtained by taking the time derivative of the loop closure equation, eq. (3-1), and noting that the time derivatives of θ_i, and $\bar{X}$ equals $\bar{\omega}_i$ and $\bar{V}_{41}$, respectively. The time derivative of eq. (3-1) is

$$i\,\bar{R}_{L2}\,\bar{\omega}_2\,e^{i\theta_2} + i\,\bar{R}_{L3}\,\bar{\omega}_3\,e^{i\theta_3} = \bar{V}_{41}e^{i0} \tag{3-4}$$

Again, by separating eq. (3-4) into its real and imaginary components and simplifying, the following are obtained.

$$\bar{\omega}_3 = -\frac{\bar{R}_{L2}\cos\theta_2}{\bar{R}_{L3}\cos\theta_3}\,\bar{\omega}_2 \tag{3-5}$$

$$\bar{V}_{41} = -\bar{R}_{L2}\,\bar{\omega}_2\sin\theta_2 - \bar{R}_{L3}\,\bar{\omega}_3\sin\theta_3 \tag{3-6}$$

By taking the time derivative of eq. (3-4) and defining $\bar{\alpha}_i$ and $\bar{A}_{41}$ as the time derivatives of $\bar{\omega}_i$ and $\bar{V}_{41}$, respectively, the following equation is obtained

$$\bar{R}_{L2}e^{i\theta_2}(i\bar{\alpha}_2 + i^2\bar{\omega}_2^2) + \bar{R}_{L3}e^{i\theta_3}(i\bar{\alpha}_3 + i^2\bar{\omega}_3^2) = \bar{A}_{41}e^{i0} \tag{3-7}$$

Separating eq. (3-7) into its real and imaginary components and simplifying obtains the following results

$$\bar{\alpha}_3 = \frac{\bar{\omega}_3}{\bar{\omega}_2}\bar{\alpha}_2 + \frac{\bar{R}_{L2}\bar{\omega}_2^2\sin\theta_2 + \bar{R}_{L3}\bar{\omega}_3^2\sin\theta_3}{\bar{R}_{L3}\cos\theta_3} \tag{3-8}$$

$$\bar{A}_{41} = -\bar{R}_{L2}(\bar{\alpha}_2\sin\theta_2 + \bar{\omega}_2^2\cos\theta_2) - \bar{R}_{L3}(\bar{\alpha}_3\sin\theta_3 + \bar{\omega}_3^2\cos\theta_3) \tag{3-9}$$

Additional simplification is possible because the crank has a constant angular velocity, $\bar{\omega}_2$, whose dimensionless magnitude is 1. Since $\bar{\omega}_2$ is constant $\bar{\alpha}_2 = 0$.

To find the real and imaginary components of acceleration of the center of mass of the connecting rod the following equations are used:

$$\bar{A}_{x3} = -\bar{R}_{L2}(\bar{\alpha}_2 \sin\theta_2 + \bar{\omega}_2^2 \cos\theta_2) - \bar{R}_{LX}(\bar{\alpha}_3 \sin\theta_3 + \bar{\omega}_3^2 \cos\theta_3) \quad (3\text{-}10)$$

$$\bar{A}_{y3} = \bar{R}_{L2}(\bar{\alpha}_2 \cos\theta_2 - \bar{\omega}_2 \sin\theta_2) + \bar{R}_{LX}(\bar{\alpha}_3 \cos\theta_3 - \bar{\omega}_3^2 \sin\theta_3) \quad (3\text{-}11)$$

where $\bar{A}_{x3}$ and $\bar{A}_{y3}$ are the linear acceleration components in the real and imaginary directions of the center mass of the connecting rod located a distance $\bar{R}_{LX}$ from the pin connecting the crank and connecting rod.

3-2 Dynamic-Force Model with Massless Bearings

This model of the force and torques transmitted by the mechanism includes the effects of coulomb friction, inertia forces, and external load. The external load is applied to the piston along its line of motion. The friction effects occur where contacting members have relative motion. The inertia effects are produced by a body's mass being subjected to linear and rotational accelerations.

The model of friction effects for a sliding joint was determined to be a force opposing the relative motion between the contacting members. This force was found to be equal to

$$F_{ab} = -\mu\,|F_N|\,\mathrm{sgn}(V_{ab}) \quad (3\text{-}12)$$

where F_{ab} is the force surface b exerts on surface a (friction force), μ is the coefficient of friction, $|F_N|$ is the absolute value of the normal

force between the surfaces, and V_{ab} is the relative velocity of surface a with respect to surface b.

To model the effects of friction in the pin connections, the friction circle concept is employed. This concept is illustrated in Figure 3-3. In Figure 3-3, points A and B represent the centers of the bearing and journal, respectively, who's radii are r and R. Since the percent difference between the two radii is quite small, they are assumed to be equal for the force analysis. The reaction force, F, is the force exerted by the journal on the bearing. The reaction force has components normal to the surface, F_N, and tangential to the surface, F_T. The tangential force is a friction force that opposes the relative motion of the bearing with respect to the journal, ω. The tangential force produces a moment about B that is $R\ F_T$. The line of action of the force is tangential to a smaller circle centered at B with a radius R_F. A moment is produced that is equal to $R_F F$. By equating the moments the following relationship is developed:

$$R_F = R \frac{F_T}{F} \tag{3-13}$$

Noting that $F_T = \mu F_n$ then eq. (3-13) can be reduced to

$$R_F = R \frac{\mu}{\sqrt{\mu^2 + 1}} \tag{3-14}$$

where R_F is the friction circle radius. Note that this radius is constant as long as the bearing radius (R), and the coefficient of friction (μ) remain constant. A friction torque exerted by member i on member j (T_{ij}) is then found to be equal to

$$T_{ij} = -|F_{ij}|\ R_F\ \mathrm{sgn}(\omega_j - \omega_i) \tag{3-15}$$

where F_{ij} is the reaction force of member i acting on member j, and ω_i and

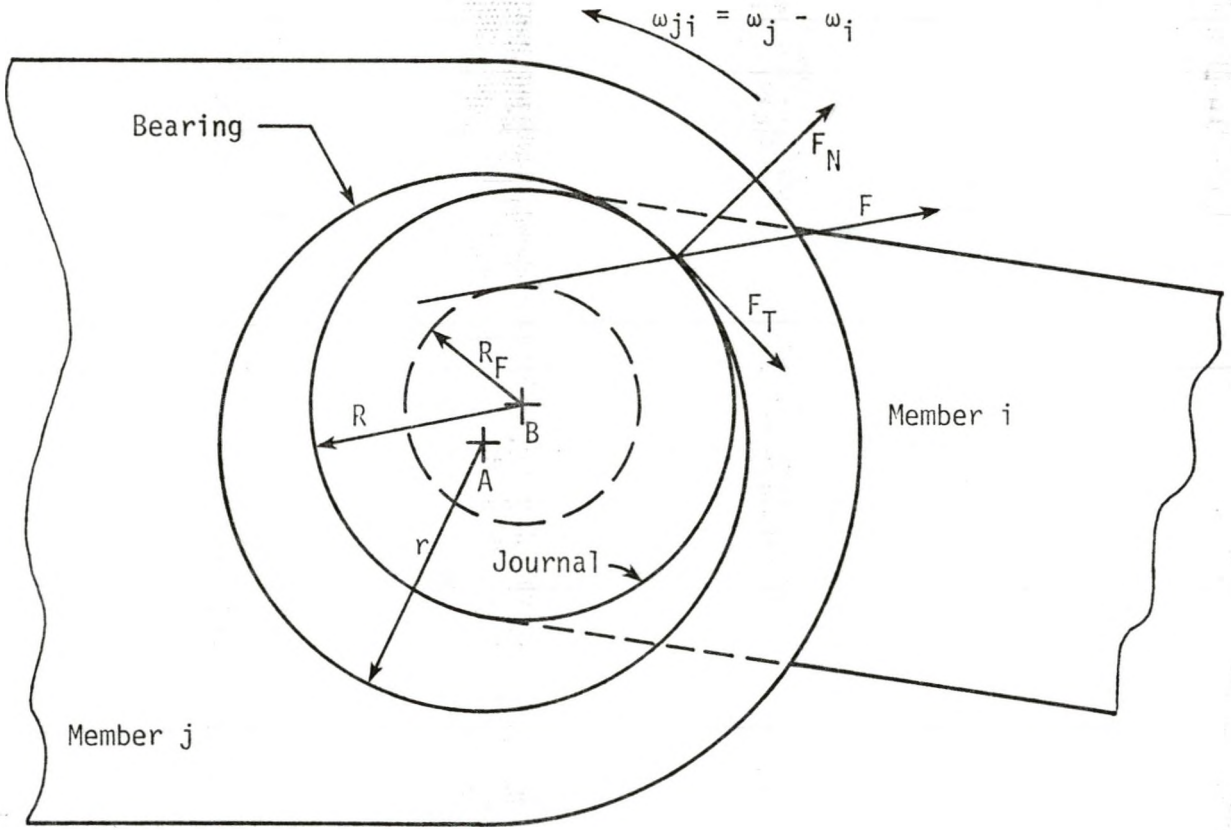

FIGURE 3-3 - ILLUSTRATION OF THE FRICTION CIRCLE CONCEPT

ω_j are the angular velocities of the two members. Figure 3-3 is redrawn in a rectangular coordinate system with the reaction force moved to the center of the journal (see Figure 3-4). The reaction is represented as a force couple. The force is represented by its components parallel to the real axis (F_{xij}) and the imaginary axis (F_{yij}). The dimensionless friction torque is:

$$\overline{T}_{ij} = -(\overline{F}_{xij}^{\,2} + \overline{F}_{yij}^{\,2})^{1/2}\, \overline{R}_F \text{ sgn } (\overline{\omega}_j - \overline{\omega}_i) \qquad (3\text{-}16)$$

To complete the dynamic force analysis, the members of the mechanism are shown as free bodies (Figure 3-5). The reaction forces are represented by their x and y components, while the torques are shown as being positive in a counter-clockwise direction. The inertia forces and torques are replaced by their D'Alembert equivalents, therefore, the sum of forces and the sum of the torques are zero for each free body. Since this is a planar mechanism, three independent equations can be developed for each link. They are the sum of the forces in the x direction equals zero, the sum of the forces in the y direction equals zero, and the sum of the moments equals zero. Also the sum of the forces in the x and y directions, and the sum of the moments equals zero for each pin. Using this fact, the following general equations are developed:

$$\begin{aligned} \overline{F}_{xij} &= -\overline{F}_{xji} \\ \overline{F}_{yij} &= -\overline{F}_{yji} \\ \overline{T}_{ij} &= -\overline{T}_{ji} \end{aligned} \qquad (3\text{-}17)$$

Analyzing the slider crank linkage, shown as free bodies in Figure 3-5, the following equations are developed for the crank, noting that it is a uniform disk rotating about its center at a constant angular velocity:

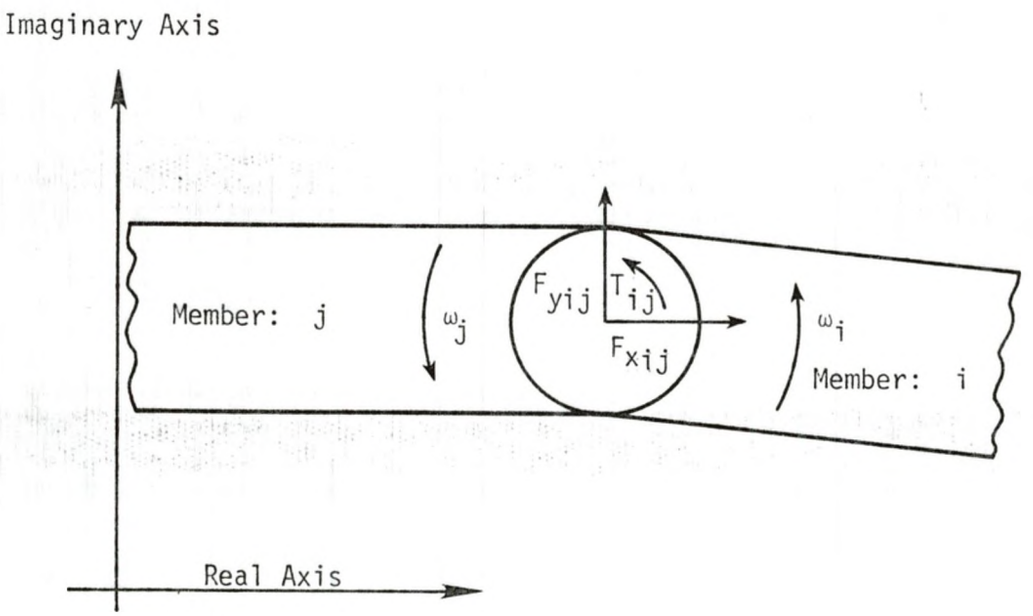

FIGURE 3-4 - BEARING FORCE IN A RECTANGULAR COORDINATE SYSTEM

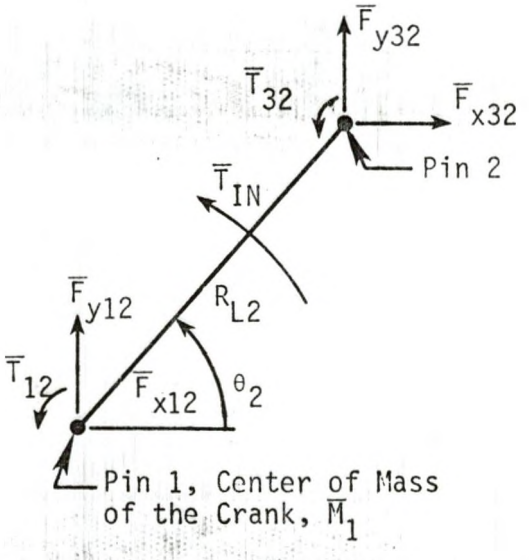

FIGURE 3-5A - FREE-BODY DIAGRAM OF THE CRANK

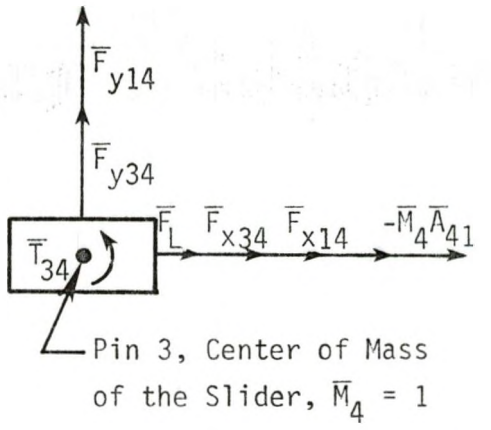

Figure 3-5B - FREE-BODY DIAGRAM OF THE SLIDER

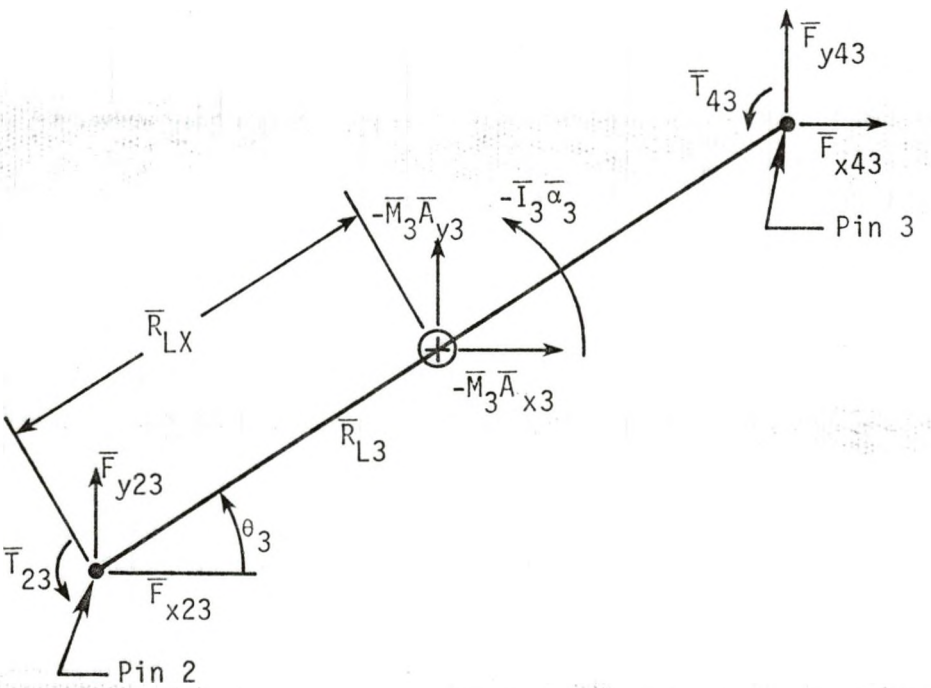

FIGURE 3-5C - FREE-BODY DIAGRAM OF THE CONNECTING ROD

$$\overline{T}_{IN} = -\overline{T}_{12} - \overline{T}_{32} + \overline{R}_{L2}\sin(\theta_2)\,\overline{F}_{x32} - \overline{R}_{L2}\cos(\theta_2)\,\overline{F}_{y32} \qquad (3\text{-}18)$$

$$\overline{F}_{x12} = -\overline{F}_{x32} \qquad (3\text{-}19)$$

$$\overline{F}_{y12} = -\overline{F}_{y32} \qquad (3\text{-}20)$$

Note that T_{IN} is the external input torque applied to the crank. Equilibrium equations for the slider are

$$\overline{F}_{x34} + \overline{F}_{L} + \overline{F}_{x14} - \overline{M}_4\,\overline{A}_{41} = 0 \qquad (3\text{-}21)$$

$$\overline{F}_{y34} + \overline{F}_{y14} = 0 \qquad (3\text{-}22)$$

where $\overline{F}_L$ is the external load and $\overline{F}_{x14}$ is the friction force the frame exerts on the slider given by

$$\overline{F}_{x14} = -|\overline{F}_{y14}|\,\mu\,\mathrm{sgn}(\overline{V}_{41}) \qquad (3\text{-}23)$$

When developing the equation for the connecting rod, note that the only mass associated with this member is that of a uniform rod. Its center of mass is located halfway between the pins, so $\overline{R}_{LX} = \overline{R}_{L3}/2$. The linear acceleration of the center of mass are given by eqs. (3-10, 11). The inertia of a uniform rod about its center of mass is

$$I = \frac{1}{12} L^3\,\rho\pi\,D^2/4 \qquad (3\text{-}24)$$

For our case, D equals L/10; then eq. (3-24) is rewritten as:

$$\overline{I}_3 = \frac{\overline{\rho\pi}}{4800}\,\overline{R}_{L3}{}^5 \qquad (3\text{-}25)$$

The mass of the connecting rod is

$$\overline{M}_3 = \overline{\rho\pi}\;\overline{R}_{L3}{}^3/400 \qquad (3\text{-}26)$$

The equilibrium equations are then

$$\overline{T}_{23} + \overline{T}_{43} - \overline{I}_3\,\overline{\alpha}_3 + \overline{M}_3\,\overline{A}_{x3}\,\frac{\overline{R}_{L3}}{2}\sin\theta_3 - \overline{M}_3\,\overline{A}_{y3}\frac{\overline{R}_{L3}}{2}\cos\theta_3 +$$

$$\overline{F}_{y43}\,\overline{R}_{L3}\cos\theta_3 - \overline{F}_{x43}\,\overline{R}_{L3}\sin\theta_3 = 0 \qquad (3\text{-}29)$$

$$\overline{F}_{x43} - \overline{M}_3\,\overline{A}_{x3} + \overline{F}_{x23} = 0 \qquad (3\text{-}28)$$

$$\overline{F}_{y43} - \overline{M}_3\,\overline{A}_{y3} + \overline{F}_{y23} = 0 \qquad (3\text{-}29)$$

The following substitutions or rearrangements of equilibrium equations are going to be substituted into the equilibrium equations (3-18, 21, 27)

$$\overline{B}_1 = \overline{M}_4\,\overline{A}_{41}$$

$$\overline{B}_2 = \overline{M}_3\,\overline{A}_{x3}$$

$$\overline{B}_3 = \overline{M}_3\,\overline{A}_{y3}$$

$$\overline{B}_4 = \overline{I}_3\,\overline{\alpha}_3$$

$$\overline{R}_{LX} = \overline{R}_{L3}/2$$

$$\overline{X} = \overline{F}_{x34} \qquad (3\text{-}30)$$

$$\overline{Y} = \overline{F}_{y34}$$

$$\overline{Z} = \overline{F}_{34} = (\overline{X}^2 + \overline{Y}^2)^{1/2}$$

$$\overline{X}' = \overline{F}_{x34} + \overline{B}_2$$

$$\overline{Y}' = \overline{F}_{y34} + \overline{B}_3$$

$$\overline{Z}' = (\overline{X'}^2 + \overline{Y'}^2)^{1/2}$$

After a few simplifications, the above equations become:

$$\bar{T}_{IN} = -\bar{Z}'(\bar{C}_1 - \bar{C}_2) + \bar{R}_{L2}\,(\bar{Y}'\cos\theta_2 - \bar{X}'\sin\theta_2) \tag{3-31}$$

$$0 = F(\bar{X},\bar{Y}) = \bar{Z}'\,\bar{C}_2 + \bar{Z}\,\bar{C}_3 + \cos\theta_3(-\bar{B}_3\,\bar{R}_{LX} - \bar{R}_{L3}\bar{Y}) + \sin\theta_3\,(\bar{B}_2\,\bar{R}_{LX} + \bar{X}\,\bar{R}_{L3}) - \bar{B}_4 \tag{3-32}$$

$$0 = G\,(\bar{X},\bar{Y}) = \bar{X} + \bar{F}_L + |\bar{Y}|\,\bar{C}_4 - \bar{B}_1 \tag{3-33}$$

Where the "C" terms are parts of the friction model and equal

$$\bar{C}_1 = -\bar{R}_1 \frac{\mu}{(\mu^2 + 1)^{1/2}} \operatorname{sgn}(\bar{\omega}_2) \tag{3-34}$$

$$\bar{C}_2 = -\bar{R}_2 \frac{\mu}{(\mu^2 + 1)^{1/2}} \operatorname{sgn}(\bar{\omega}_3 - \bar{\omega}_2) \tag{3-35}$$

$$\bar{C}_3 = -\bar{R}_3 \frac{\mu}{(\mu^2 + 1)^{1/2}} \operatorname{sgn}(\bar{\omega}_3) \tag{3-36}$$

$$\bar{C}_4 = -\mu\,\operatorname{sgn}(\bar{V}_{41}) \tag{3-37}$$

The solution to eqs. (3-31 through 33) will be shown in a later section.

3-3 Dynamic-Force Model with Journal-Bearing Masses

The difference between this analysis and the preceding analysis is that the journal-bearings have a mass associated with them. The journals or pins are attached to the crank and slider while the connecting rod and frame have the bearings attached. The pins have a radius $\bar{R}_i$ and a length of $\bar{R}_{L3}/10$. The bearing dimensions are assumed to be a length $\bar{R}_{L3}/10$, an inside diameter $\bar{R}_i$, and an outer diameter of 1.5 $\bar{R}_i$. The bearing, journal, and links have the same material density, $\bar{\rho}$. The crank is again assumed to

be rotating at a constant angular velocity about its center, which is its center of mass. Because of this assumption, eq. (3-31) is the same whether the journal-bearings have mass or not. Therefore, this section focuses on the connecting rod and slider. Figure 3-6 shows a physical representation of the connecting rod and slider.

The mass of the connecting rod is the mass of the rod plus the mass of the two bearings. The mass of the rod is

$$\bar{M}_{31} = (\bar{R}_{L3} - 1.5\ \bar{R}_2 - 1.5\ \bar{R}_3)\ \pi\bar{\rho}\ (\frac{\bar{R}_{L3}}{20})^2 \qquad (3\text{-}38)$$

and the mass of bearings 2 and 3 are

$$\bar{M}_{32} = \frac{\bar{R}_{L3}}{10}((1.5\ \bar{R}_2)^2 - \bar{R}_2{}^2)\pi\bar{\rho} \qquad (3\text{-}39)$$

$$\bar{M}_{33} = \frac{\bar{R}_{L3}}{10}\ ((1.5\ \bar{R}_3)^2 - \bar{R}_3{}^2)\pi\bar{\rho} \qquad (3\text{-}40)$$

The mass of the connecting rod is then

$$\bar{M}_3 = \bar{M}_{31} + \bar{M}_{32} + \bar{M}_{33} \qquad (3\text{-}41)$$

The center of mass is located a distance $\bar{R}_{LX}$ from the center of bearing 2. This distance is

$$\bar{R}_{LX} = [(0)\bar{M}_{32} + (1.5\ \bar{R}_2 + (\bar{R}_{L3} - 1.5\ \bar{R}_2 - 1.5\ \bar{R}_3)/2)\bar{M}_{31} + \bar{R}_{L3}\bar{M}_{33}]/\bar{M}_3 \qquad (3\text{-}42)$$

The inertia about the center of mass is given by

$$\bar{I}_3 = ((1.5\ \bar{R}_2)^4 - \bar{R}_2{}^4)\ \frac{\pi}{2}\ \frac{\bar{R}_{L3}}{10}\ \bar{\rho} + \bar{M}_{32}\ \bar{R}_X{}^2 +$$

$$(\frac{\bar{R}_{L3}}{20})^2\ \bar{\rho}\ \pi(\bar{R}_{L3} - 1.5\ \bar{R}_2 - 1.5\ \bar{R}_3)^3 + \bar{M}_{31}\ ((\bar{R}_{L3} - 1.5\ \bar{R}_2 - 1.5\ \bar{R}_3)/2 +$$

$$1.5\ \bar{R}_2 - \bar{R}_{LX})^2 + ((1.5\ \bar{R}_3)^4 - \bar{R}_3{}^4)\ \frac{\pi}{2}\ \frac{\bar{R}_{L3}}{10}\ \bar{\rho} + \bar{M}_{33}\ (\bar{R}_{L3} - \bar{R}_{LX})^2 \qquad (3\text{-}43)$$

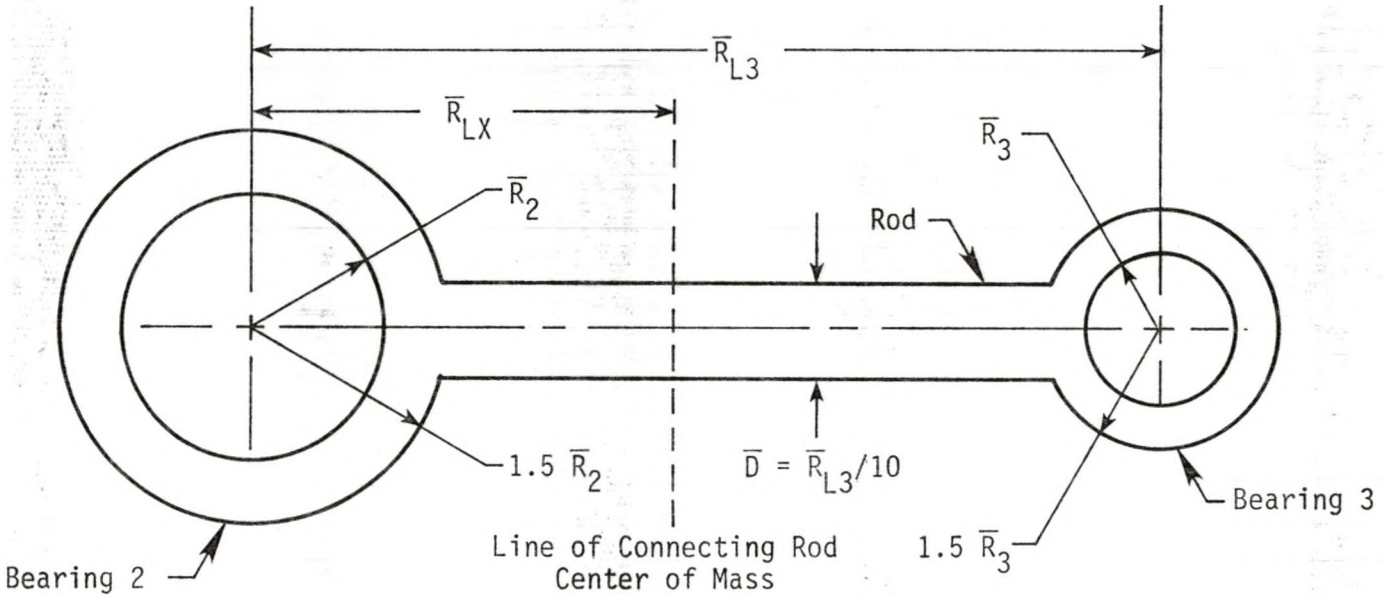

FIGURE 3-6A - PHYSICAL SHAPE OF THE CONNECTING ROD

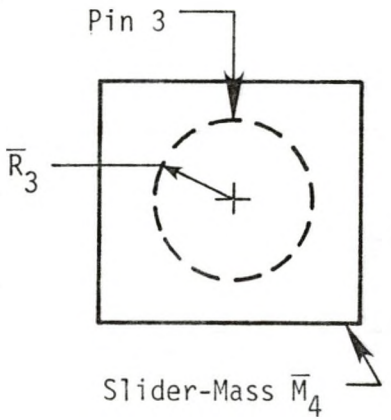

FIGURE 3-6B - PHYSICAL REPRESENTATION OF THE SLIDER AND PIN

The mass of the piston is now the slider mass plus the pin mass, or

$$\overline{M}_4' = \overline{M}_4 + \overline{\rho\pi}\,\frac{\overline{R}_{L3}}{10}\,(\overline{R}_3)^2 \tag{3-44}$$

Substituting these values into $\overline{B}_1$, $\overline{B}_2$, $\overline{B}_3$, $\overline{B}_4$, $\overline{R}_{LX}$ of eq. (3-30) equations of the form of eqs. (3-31 through 33) are obtained for the dynamic-force analysis with journal-bearing masses.

3-4 Force Solutions

Since eq. (3-32, 33) are in a nonlinear form to solve for the reaction force components $\overline{X}$ and $\overline{Y}$, an iterative technique is used. Eqs. (3-32, 33) are equal to zero and shall be represented by $F(\overline{X},\overline{Y})$ and $G(\overline{X},\overline{Y})$, respectively. The following series approximation of $F(X,Y)$ and $G(X,Y)$ are made (Newton Method)

$$0 = F(\overline{X},\overline{Y}) \simeq F(\overline{X}_n,\overline{Y}_n) + \frac{\partial F(\overline{X}_n,\overline{Y}_n)}{\partial \overline{X}}\,(\overline{X}_{n+1} - \overline{X}_n) + \frac{\partial F(\overline{X}_n,\overline{Y}_n)}{\partial \overline{Y}}\,(\overline{Y}_{n+1} - \overline{Y}_n) \tag{3-45}$$

$$0 = G(\overline{X},\overline{Y}) \simeq G(\overline{X}_n,\overline{Y}_n) + \frac{\partial G(\overline{X}_n,\overline{Y}_n)}{\partial \overline{X}}\,(\overline{X}_{n+1} - \overline{X}_n) + \frac{\partial G(\overline{X}_n,\overline{Y}_n)}{\partial \overline{Y}}\,(\overline{Y}_{n+1} - \overline{Y}_n) \tag{3-46}$$

where $\overline{X}_n$ and $\overline{Y}_n$ are the n^{th} approximation of the actual values of $\overline{X}$ and $\overline{Y}$ while $G(\overline{X}_n,\overline{Y}_n)$ and $F(\overline{X}_n,\overline{Y}_n)$ are the n^{th} approximation of $G(\overline{X},\overline{Y})$ and $F(\overline{X},\overline{Y})$. Eqs. (3-45, 46) are then solved and the following iterative equations are obtained

$$\overline{X}_{n+1} = \overline{X}_n + \frac{F(\overline{X}_n,\overline{Y}_n)\;\dfrac{\partial G(\overline{X}_n,\overline{Y}_n)}{\partial \overline{Y}} - G(\overline{X}_n,\overline{Y}_n)\;\dfrac{\partial F(\overline{X}_n,\overline{Y}_n)}{\partial \overline{Y}}}{\dfrac{\partial F(\overline{X}_n,\overline{Y}_n)}{\partial \overline{Y}}\;\dfrac{\partial G(\overline{X}_n,\overline{Y}_n)}{\partial \overline{X}} - \dfrac{\partial F(\overline{X}_n,\overline{Y}_n)}{\partial \overline{X}}\;\dfrac{\partial G(\overline{X}_n,\overline{Y}_n)}{\partial \overline{Y}}} \tag{3-47}$$

$$\bar{Y}_{n+1} = \bar{Y}_n + \frac{G(\bar{X}_n,\bar{Y}_n)\ \frac{\partial F(\bar{X}_n,\bar{Y}_n)}{\partial \bar{X}} - F(\bar{X}_n,\bar{Y}_n)\ \frac{\partial G(\bar{X}_n,\bar{Y}_n)}{\partial \bar{X}}}{\frac{\partial F(\bar{X}_n,\bar{Y}_n)}{\partial \bar{Y}}\ \frac{\partial G(\bar{X}_n,\bar{Y}_n)}{\partial \bar{X}} - \frac{\partial F(\bar{X}_n,\bar{Y}_n)}{\partial \bar{X}}\ \frac{\partial G(\bar{X}_n,\bar{Y}_n)}{\partial \bar{Y}}} \qquad (3\text{-}48)$$

Initial guesses of $\bar{X}$ and $\bar{Y}$ are required, then eqs. (3-47, 48) are used until $\bar{X}_{n+1} - \bar{X}_n$ and $\bar{Y}_{n+1} - \bar{Y}_n$ become close enough to zero. The values of $\bar{X}_n$, and $\bar{Y}_n$ are then substituted into eqs. (3-30, 31) for $\bar{X}$ and $\bar{Y}$ to find an approximate value of $\bar{T}_{IN}$, and the bearing forces $\bar{Z}$ and $\bar{Z}'$. Values of $\bar{T}_{IN}$, $\bar{Z}$, and $\bar{Z}'$ are calculated for equally spaced rotations of the crank. An outline of the method is now detailed below.

1. Complete the kinematic analysis and calculation of all constants for the given crank position.
2. Assume initial values $\bar{X}_1$, $\bar{Y}_1$.
3. Calculate initial values of $\bar{X}_n'$, $\bar{Y}_n'$, $\bar{Z}_n'$, $\bar{Z}_n$.
4. Calculate $F_n = F(\bar{X}_n,\bar{Y}_n)$, and $G_n = G(\bar{X}_n,\bar{Y}_n)$

$$F(\bar{X}_n,\bar{Y}_n) = \bar{Z}'\ \bar{C}_2 + \bar{Z}\ C_3 + \cos\theta_3\ (-\bar{B}_3\ \bar{R}_{LX} - \bar{R}_{L3}\ \bar{Y}) + \sin\theta_3\ (\bar{B}_2\ \bar{R}_{LX} + \bar{X}\ \bar{R}_{L3}) - \bar{B}_4 \qquad (3\text{-}49)$$

$$G(\bar{X}_n,\bar{Y}_n) = \bar{X} + \bar{F}_L + |\bar{Y}|\ \bar{C}_4 - \bar{B}_1 \qquad (3\text{-}50)$$

5. Calculate $\frac{\partial F_n}{\partial X}$, $\frac{\partial F_n}{\partial Y}$, $\frac{\partial G_n}{\partial X}$, $\frac{\partial G_n}{\partial Y}$

$$\frac{\partial F_n}{\partial X} = \bar{R}_{L3}\sin\theta_3 - \bar{C}_2\ \bar{X}/\bar{Z} + \bar{C}_3\ \bar{X}'/\bar{Z}' \qquad (3\text{-}51)$$

$$\frac{\partial F_n}{\partial Y} = \bar{R}_{L3}\cos\theta_3 - \bar{C}_2\ \bar{Y}/\bar{Z} + \bar{C}_3\ \bar{Y}'/\bar{Z}' \qquad (3\text{-}52)$$

$$\frac{\partial G_n}{\partial X} = 1$$

$$\frac{\partial G_n}{\partial \bar{Y}} = \begin{cases} \bar{C}_4 & \text{if } \bar{Y} > 0 \\ 0 & \text{if } \bar{Y} = 0 \\ -\bar{C}_4 & \text{if } \bar{Y} < 0 \end{cases} \qquad (3\text{-}53)$$

6. Calculate $\bar{X}_{n+1}$, $\bar{Y}_{n+1}$ by eqs. (3-47, 48)

7. If $\bar{X}_{n+1} - \bar{X}_n$ and $\bar{Y}_{n+1} - \bar{Y}_n$ are within some interval bounding zero, go to Step 9.

8. Loop back to Step 3.

9. Calculate $\bar{T}_{in}$

$$\bar{T}_{in} = (\bar{Y}')\bar{R}_{L2} \cos \theta_2 - (\bar{X}')\bar{R}_{L2} \sin \theta_2 - \bar{Z}'(\bar{C}_1 - \bar{C}_2) \qquad (3\text{-}54)$$

10. Rotate the crank to it's new position and start over from Step 1.

3-5 Objective Function

As previously stated, the objective function is a combination of the input work and shear stress. The input work $\bar{W}$ is expressed exactly by the following equation

$$\bar{W} = \int_0^{2\pi} \bar{T}_{IN} \, d\theta_2 \qquad (3\text{-}55)$$

This integral can be approximated as follows:

$$\bar{W} = \sum_1^N \bar{T}_{IN} \, \Delta\theta \qquad (3\text{-}56)$$

Where $\bar{T}_{IN}$ are the input torques for crank positions a distance $\Delta\theta$ apart, and N is the number an increment of crank rotation needs to complete the cycle. The bearing shear stress is represented by the stress factor, $\bar{\beta}$. Discrete values of $\bar{\beta}$ are determined for each crank position and used to approximate the maximum shear stress. Obviously, the accuracy of the approximation decreases with increasing $\Delta\theta$.

CHAPTER 4

OPTIMIZATION OF THE SLIDER-CRANK MECHANISM

The slider-crank mechanism is optimized on the basis of performance criteria related to the required cycle input work and the maximum bearing shear stress. These criteria tend to be competing objectives. For example, it appears that increasing the bearing radii will decrease the associated shear stress, but as the bearing becomes larger the friction torque increases which increases the cycle input work. Therefore, to establish the trade offs between these quantities the following objective function is used:

$$f = \overline{W} + w\,\overline{\beta}_m \qquad (4\text{-}1)$$

where f is the objective function, $\overline{W}$ is the dimensionless cycle input work, $\overline{\beta}_m$ is the largest of the maximum dimensionless stress factors associated with each bearing during a complete cycle, and w is a weighting factor which adjusts the relative merit of work and stress in the optimization process. Throughout the remainder of this thesis the dimensionless cycle input work and the maximum cyclic dimensionless stress factor are simply referred to as the work and stress factor, respectively.

A brief examination of eq. (4-1) reveals the effect of the weighting factor on the optimization process. Very large values of w tend to minimize the stress factor with little regard to the work, while values of w approaching zero tend to minimize the work with little regard to the stress factor. Values of w between the extremes produce an optimum that reflects the effects of both the work and stress factor.

The design variables for the optimization are the linkage dimensions $\overline{R}_{L2}$, $\overline{R}_{L3}$, $\overline{H}$, $\overline{R}_1$, $\overline{R}_2$, and $\overline{R}_3$. Since the stroke is held constant for all mechanism configurations, $\overline{R}_{L2}$ is computed from $\overline{R}_{L3}$ and $\overline{H}$ by eq. (2-16). From eqs. (3-19, 20) it can be shown that the reaction forces for bearings 1 and 2 have the same magnitude. Since the optimization minimizes the maximum stress factor; the stress factors for the individual bearings should be equal at the optimum. Therefore, $\overline{R}_1 = \overline{R}_2$ for the optimization process since this makes the stress factors for these bearings equal.

Thus, the mathematical optimization problem can be stated as follows.

$$\begin{aligned} &\text{minimize} && f = \overline{W} + w\,\overline{\beta}_m \\ &\text{with respect to} && \overline{R}_{L3},\ \overline{H},\ \overline{R}_1 = \overline{R}_2,\ \overline{R}_3 \end{aligned} \tag{4-2}$$

The optimization was evaluated with the aid of an optimization package developed by Afimiwala and Mayne [12]. The specific technique used is the variable metric search also referred to as the Davidon-Fletcher-Powell method [13].

4-1 Optimization Procedure

In this thesis the slider-crank mechanism is loaded as a single acting compressor. Since this is a numerical model, numerical values must be assigned to all parameters. Therefore, throughout the remainder of this thesis the following numerical values are assigned to the dimensionless quantities used to model the compression cycle:

$$\overline{P}_e = 7.65$$

$$\overline{P}_i = \overline{P}_a = 1.93$$

$$k = 1.4$$

$$\gamma = 0.1$$

$$\overline{A}_p = 0.35$$

The following numerical values or relationships are assigned to dimensionless mechanism parameters of mass density ($\overline{\rho}$), connecting rod diameter ($\overline{D}$), and bearing length ($\overline{L}$).

$$\overline{\rho} = 12.3$$

$$\overline{D} = \overline{R}_{L3}/10$$

$$\overline{L} = \overline{D}$$

Two other factors need to be studied before the optimization process can be started. The factors are the size of the increment of crank rotation and the accuracy of the approximation of the reaction forces. The smaller increment of crank rotation and larger accuracy in approximation of the reaction forces improves the model's prediction of the work and stress factor. This highly accurate model is obtained at the expense of computing time, the higher the accuracy the larger the computing time. By analyzing the effects of single parameter variation, it was determined that a 6° increment is sufficient. Also, by performing the iterative technique used to determine the reaction forces four times, the error in the approximation was less than 0.001 percent for all cases considered. These values are sufficient if the optimization process is divided into two steps. The first step is the optimization of the inline slider-crank mechanism, with the offset equal to zero. Once this is completed and an optimum mechanism is determined, the offset is adjusted to attempt to further minimize the

objective function. This division was determined to be necessary by analyzing a plot of stress factor versus offset (Figure 4-1). The curve produced is jagged and tends to smooth as the increment of crank angle rotation is decreased from 6° to $1/2^{\circ}$. The stress factors as a function of $\overline{H}$ should be the smooth curves drawn through all the points of relative maximums. This curve corresponds to an increment of crank rotation approaching zero. To produce this curve would take an extremely large amount of computing time. A smooth curve is required otherwise the optimization process picks some false location at the base of any one of the jogs. The curves for stress factor versus any of the other parameters were smooth. Therefore, the optimization statement now becomes first

$$\begin{aligned} &\text{minimize} && f = \overline{W} + w\overline{\beta} \\ &\text{with respect to} && \overline{R}_{L3},\ \overline{R}_1 = \overline{R}_2,\ \overline{R}_3,\ \overline{H} = 0 \end{aligned} \tag{4-3}$$

and secondly,

$$\begin{aligned} &\text{minimize} && f = \overline{W} + w\overline{\beta} \\ &\text{with respect to} && \overline{H} \end{aligned} \tag{4-4}$$

The tradeoffs that are recognized to exist for the optimization statement given by eqs. (4-3, 4) are enumerated as follows:

1. The trade offs incurred by $\overline{R}_1$:
   a. Increasing $\overline{R}_1$ increases the friction torque which increases the work as shown by eq. (3-18).
   b. Increasing $\overline{R}_1$ increases the area bearing the reaction force which decreases the associated stress factor, as shown by eq. (2-19).
2. The trade offs occurring for $\overline{R}_2$:
   a. Increasing $\overline{R}_2$ increases the bearing area which decreases the associated stress factor.

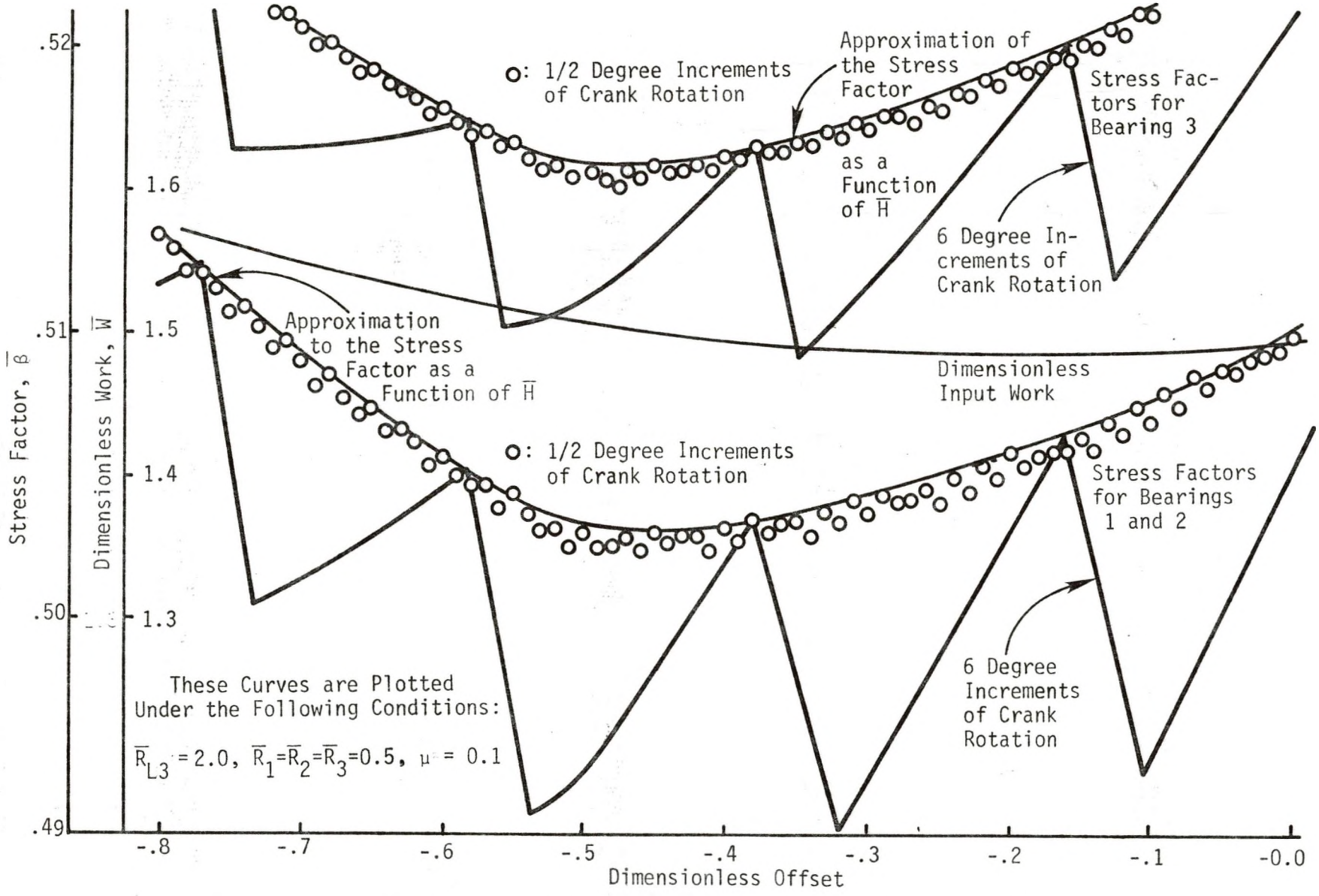

FIGURE 4-1 - INPUT WORK AND STRESS FACTOR VERSUS OFFSET

b. Increasing $\overline{R}_2$ increases the bearing mass which increases the inertia forces.

c. Increasing $\overline{R}_2$ increases the friction torque which increases the work.

d. Increasing $\overline{R}_2$ increases the friction torque which changes the reaction forces as given by eq. (3-27).

3. The trade offs existing for $\overline{R}_3$:

a. Increasing $\overline{R}_3$ decreases the associated stress factor.

b. Increasing $\overline{R}_3$ increases the inertia forces.

c. Increases in $\overline{R}_3$ increase the friction torque which changes the reaction forces.

4. The trade offs for $\overline{R}_{L3}$:

a. Increasing $\overline{R}_{L3}$ increases the connecting rod mass which increase the inertia forces.

b. Increasing $\overline{R}_{L3}$ reduces the magnitudes of the connecting rod velocity and acceleration which decreases the inertia forces.

c. The bearing lengths are proportional to the connecting rod length. Increases in connecting rod length then increase the bearing area, reduce the stress factor, and increase the bearing mass, increasing the inertia effects.

d. Increases in $\overline{R}_{L3}$ tend to align the connecting rod with the direction of slider motion. If they are aligned the y component of the reaction force would be reduced which reduces the reaction forces, and hence, the stress factors are also reduced. Also decreasing the y component of the forces reduces the normal force at the sliding contact. This reduction decreases the effects of friction acting upon the slider.

5. The trade offs that exist for $\overline{H}$:

a. Varying $\overline{H}$ from zero tends to increase the maximum angle between the connecting rod and direction of slider motion. There is then an increase in the y component of the reaction forces and an associated increase in the friction effects.

b. The inertia forces may align themselves so as to oppose the applied force over some region of the cycle, and by varying $\overline{H}$, a more uniform stress throughout the entire cycle may be obtained.

The following should be noted in conjunction with the trade offs mentioned. First, friction is a nonconservative effect; addition of friction automatically increases the required input work. Second, if there is no friction the inertia effects are conservative, the work will not change but the reaction forces do change. Third, the inertia effects for the connecting rod initially decrease when the connecting rod is increased from its minimum length. This decrease is due to the rapid decrease in its acceleration. Further increase in length increases the inertia effects because the connecting rod mass is increasing faster than the acceleration is decreasing.

To study the effects of the trade offs various cases of the slider-crank are analyzed. The cases start from the simplest, no friction or inertia effects, and proceed to the most complex case, complete friction and inertia effects. For the simplest case, no friction or inertia effects, the work is 0.949, and is the same for all mechanism configurations for this case. This is the amount of work required to complete a compression cycle. It was determined by evaluating the following integral:

$$\overline{W} = \oint (\overline{P}_a - \overline{P})\overline{A}_p \, dx = 0.949 \qquad (4\text{-}4)$$

This is the minimum work that any mechanism loaded by this compression cycle can have. Since there is no friction or inertia effects the bearings will approach an infinite diameter and therefore all the stress factors are zero.

4-2 Optimization Results for Special Cases

The results for the case when there are no inertia effects present are given in Table 4-1 and Figure 4-2. For this data the coefficient of friction is 0.5. Figure 4-2 shows the trade off curves relating the stress

TABLE 4-1

OPTIMIZATION RESULTS FOR THE CASE OF NO INERTIA EFFECTS AND A COEFFICIENT OF FRICTION EQUAL TO 0.5

w	$\bar{W}$	$\bar{\beta}_1 = \bar{\beta}_2$	$\bar{\beta}_3$	$\bar{R}_{L3}$*	$\bar{R}_1 = \bar{R}_2$	$\bar{R}_3$
0.01	.962	2.67	2.67	∞	0.00360	0.00360
0.1	1.01	1.24	1.24	∞	0.0167	0.0167
0.5	1.13	.723	.723	∞	0.0491	0.0491
1.0	1.23	0.574	0.574	∞	0.0779	0.0779
5.0	1.79	0.336	0.336	∞	0.228	0.228
10.0	2.28	0.266	0.266	∞	0.361	0.361
100.	7.12	0.124	0.124	∞	1.68	1.68

* These are not values generated by the optimization. It was observed that $\bar{R}_{L3}$ tended to increase without bound, therefore the model was modified to account for an infinitely long connecting rod.

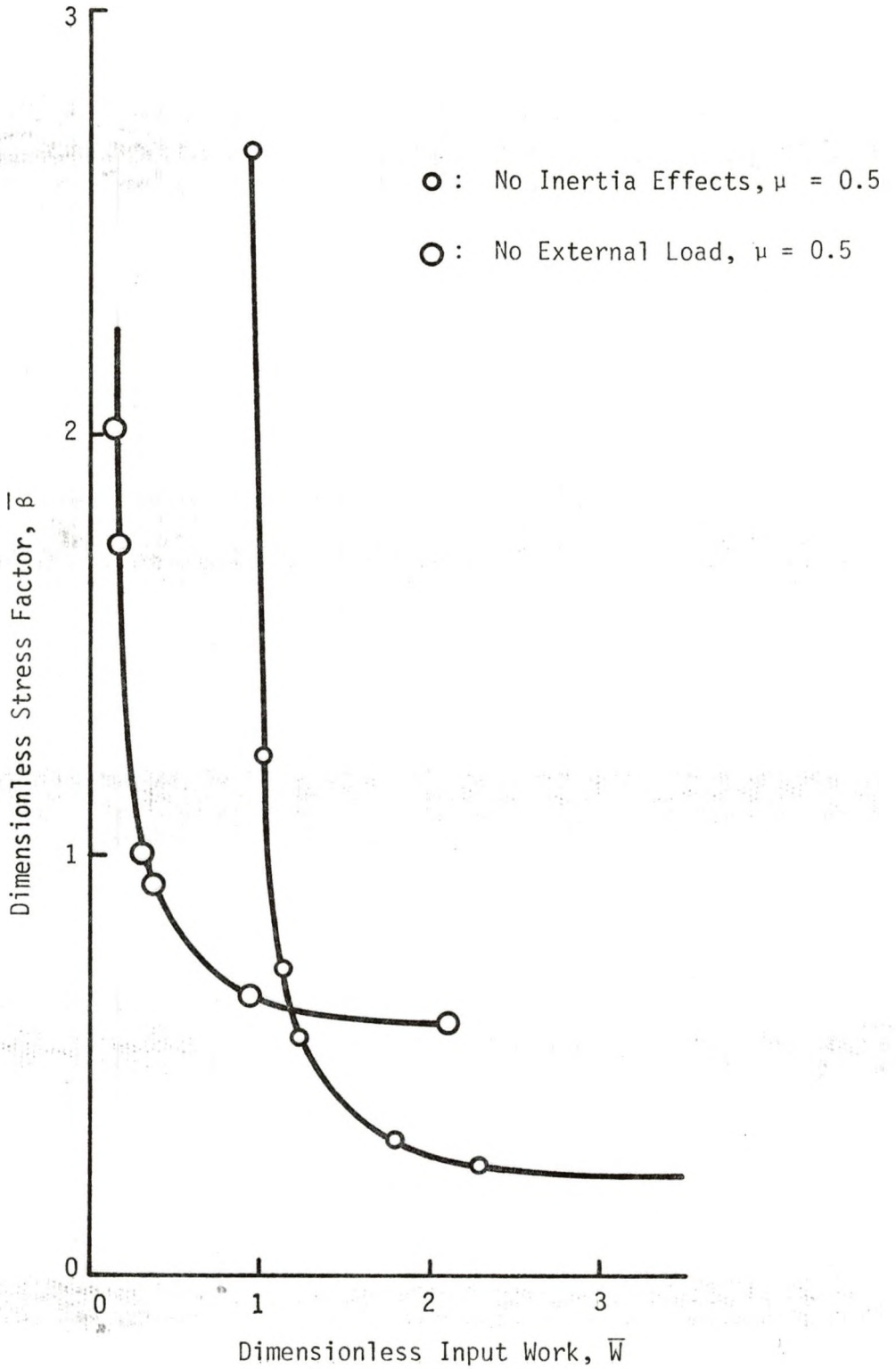

FIGURE 4-2 - OPTIMIZATION RESULTS FOR THE CASES OF NO INERTIA EFFECTS, AND NO EXTERNAL LOAD

factor and the work, where each point represents a different mechanism. A number of these mechanisms are given in Table 4-1. The values tabulated are the weighting factor, the work, stress factors, and the mechanism dimensions. First note that all the connecting rod lengths are infinite; since the connecting rod has no mass there is no penalty for its large length, but the large length cause the "y" component of the forces to be zero. Since the length of the bearing is proportional to the length of the connecting rod it was set equal to one, otherwise it would have an infinite length. Since there are no inertia effects the reaction forces for all of the bearings are identical. Since the optimum mechanism has the same stress factor for all the bearings, the bearing radii are equal.

A 90 percent reduction in the stress factor (from 2.67 to 0.266) can be obtained at the expense of a 137 percent increase in the work, but to obtain another 50 percent reduction (from 0.266 to 0.124) a 212 percent increase in the work is incurred. This is shown in Figure 4-2 as the curve switches from nearly vertical to nearly horizontal. This break in the curve occurs because the friction torques are becoming significant. The friction torque is directly related to the reaction force and the bearing radius. The reaction force for any given crank position is constant for all mechanisms. Therefore, as the bearing radii increase so does the friction torque and hence, the friction work. Since the input torque is the sum of the friction torques for bearings 1 and 2, and the torque produced by the applied load, then the input work is directly related to the bearing radii. The stress factors vary as $R^{-1/2}$ since the reaction forces are independent of the bearing radii for this case. These relationships account for the characteristic shape of the curves.

The next case considered is that of no external load but there are inertia and friction effects. The results for this case are shown in Figure 4-2 and Table 4-2. The values tabulated in Table 4-2 are the weighting factor, the work, the stress factors, and crank angle at which they occurred, θ, and the mechanism dimensions. Again it is noted that, as suspected, the stress factors are approximately the same for all bearings. The radii for bearings 1 and 2 are greater than the radius of bearing 3 for all the cases. This indicates that the inertia effects of the connecting rod increase the reaction forces at bearing 1 and 2. For cases when w is greater than or equal to five, the maximum stress factors for all the bearings no longer occur at the same position. Observing the ratio of $\bar{R}_1/\bar{R}_3$ on either side of this change in position, it is determined to be 1.3 to 1.4 for w less than 5 and 1.7 to 2.0 for w greater than or equal to 5. This indicates a rather large change in the relative magnitudes of the reaction forces when the position of maximum stresses are no longer the same. The inertia effects due to the connecting rod are predominating over the inertia effects due to the slider pin combination. The minimum stress factor obtainable for this case is 0.596. No further reduction in stress factor could be produced. At this point any further increase in any of the dimensions to reduce reaction forces or to increase the bearing area increases the mass and inertial effects enough so that an increase in the stress factor occurs. Also, increases in the bearing radius increase the friction torques and reaction forces.

The next case considered is that of a frictionless mechanism loaded by the compression cycle and inertia effects. Since the mechanism is frictionless, the work for all possible configurations is 0.949. The results of the optimization are:

TABLE 4-2

OPTIMIZATION RESULTS FOR THE CASE OF NO EXTERNAL LOAD AND A COEFFICIENT OF FRICTION EQUAL TO 0.5

w	$\overline{W}$	$\overline{\beta}_1 = \overline{\beta}_2$	$\theta^\circ(\overline{\beta}_1 = \beta_2)$	$\overline{\beta}_3$	$\theta^\circ(\overline{\beta}_3)$	$\overline{R}_{L3}$	$\overline{R}_1 = \overline{R}_2$	$\overline{R}_3$
0.05	0.155	2.03	6	2.03	6	1.50	0.0185	0.0142
0.1	0.185	1.60	6	1.60	6	1.50	0.0299	0.0230
0.5	0.301	1.04	6	1.04	6	1.71	0.0695	0.0466
1	0.364	0.929	6	0.930	6	1.69	0.0874	0.0606
5	0.945	0.665	12	0.665	6	1.88	0.202	0.118
50	2.07	0.596	12	0.596	6	2.01	0.318	0.155

$$\overline{\beta}_1 = \overline{\beta}_2 = 0.595$$

$$\overline{\beta}_3 = 0.595$$

$$\overline{R}_{L3} = 2.02$$

$$\overline{R}_1 = \overline{R}_2 = 0.619$$

$$\overline{R}_3 = 0.336$$

It is interesting to note that the minimum obtainable stress for this case and that for the case of no external load are approximately the same. The optimum mechanisms have approximately the same connecting rod lengths but the bearing radii are approximately a factor or two larger for the frictionless case.

4-3 Optimization Results When the Bearings are Massless

To determine the effect of the friction torques on the optimum mechanism the case is considered where the external compression load is applied, there are friction effects at all the joints, and inertia effects are considered except those due to the bearings. The journal and bearings are assumed to be massless. The results for this case are graphically displayed in Figure 4-3 and are tabulated in Tables 4-3 and 4-4. Table 4-3 and Table 4-4 consider the cases when the coefficient of friction is 0.1 and 0.5, respectively. Both tables contain the following data: the weighting factor, the work, the maximum stress factors and angular crank positions at which they occur, and the mechanism dimensions. In Figure 4-3 one of the points does not fall on the smooth line connecting the remaining points. The mechanism that generated this point has the following characteristics: $\overline{W} = 3.55$, $\overline{\beta}_1 = \overline{\beta}_1 = 0.515$, and $\overline{\beta}_3 = 0.629$, from Table 4-4. Notice that

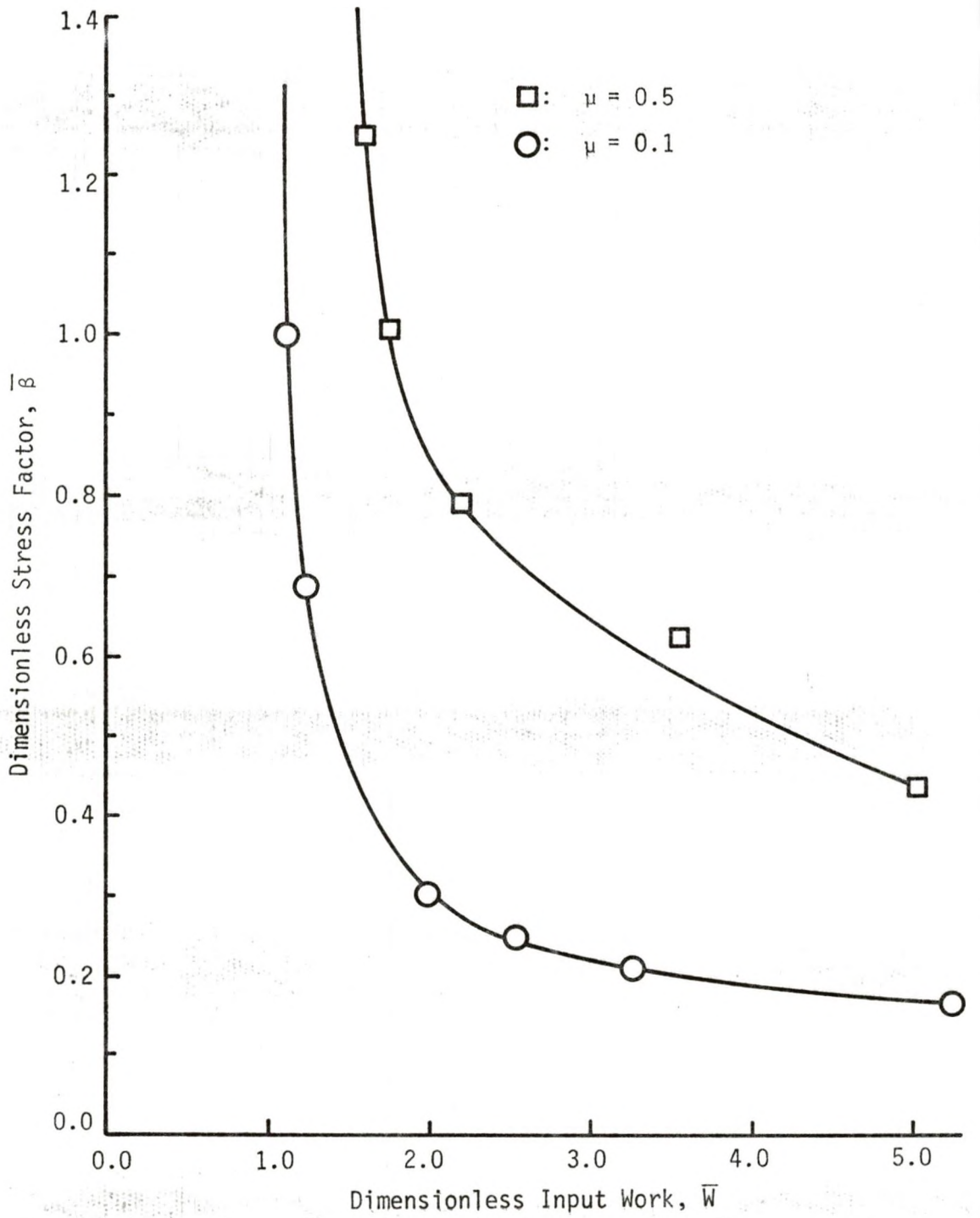

FIGURE 4-3 - OPTIMIZATION RESULTS FOR THE CASE WHEN THE BEARINGS ARE MASSLESS

TABLE 4-3

OPTIMIZATION RESULTS FOR THE CASE OF MASSLESS BEARINGS AND A COEFFICIENT OF FRICTION EQUAL TO 0.1

w	$\overline{W}$	$\overline{\beta}_1=\overline{\beta}_2$	$\theta^\circ(\overline{\beta}_1=\overline{\beta}_2)$	$\overline{\beta}_3$	$\theta^\circ(\overline{\beta}_3)$	$\overline{R}_{L3}$	$\overline{R}_1=\overline{R}_2$	$\overline{R}_3$
0.225	1.12	0.999	300	1.00	300	2.25	0.109	0.121
0.676	1.21	0.690	300	0.809	300	2.31	0.221	0.248
0.902	2.00	0.305	294	0.305	300	2.87	0.806	1.00
1.8	2.54	0.251	294	0.251	300	2.89	1.20	1.47
22.5	3.28	0.209	294	0.209	300	2.92	1.74	2.11
225.	5.23	0.165	276	0.165	276	3.04	2.98	3.32
3375.	9.22	0.127	276	0.127	276	3.12	5.25	5.71

TABLE 4-4

OPTIMIZATION RESULTS FOR THE CASE OF MASSLESS BEARINGS AND A COEFFICIENT OF FRICTION EQUAL TO .5

w	$\overline{W}$	$\overline{\beta}_1=\overline{\beta}_2$	$\theta^\circ(\overline{\beta}_1=\overline{\beta}_2)$	$\overline{\beta}_3$	$\theta^\circ(\overline{\beta}_3)$	$\overline{R}_{L3}$	$\overline{R}_1=\overline{R}_2$	$\overline{R}_3$
0.675	1.60	1.25	300	1.26	300	2.25	0.0718	0.0789
1.8	1.75	1.06	300	1.06	300	2.50	0.0869	0.0998
2.25	2.20	0.798	294	0.789	300	2.90	0.129	0.161
6.75	3.55	0.515	294	0.629	300	2.94	0.324	0.263
27	4.97	0.437	294	0.440	300	2.97	0.497	0.588
180	7.17	0.373	294	0.397	294	3.15	0.699	0.751

all of the stress factors are not the same, therefore the optimization process did not fully converge. If $\overline{R}_1$ and $\overline{R}_2$ were reduced, $\overline{\beta}_1$ and $\overline{\beta}_2$ would increase, and the friction torque would be reduced with the net effect of reducing the work. To prove this, the same mechanism was analyzed except $\overline{R}_1 = R_2 = .280$ instead of 0.324. The work was reduced 8 percent to 3.25, $\overline{\beta}_1$ and $\overline{\beta}_2$ increased 7 percent to 0.551, and $\overline{\beta}_3$ showed a slight reduction to 0.627 for a 14 percent decrease in $\overline{R}_1$ and $\overline{R}_2$. This moves the point closer to the curve.

A general observation from Tables 4-3 and 4-4 is that when the work is the dominant term in the objective function, the connecting rod length tends to be shorter. When the stress factor dominates, large values of $\overline{W}$ occur and, the connecting length increases. This suggests that the shorter connecting rod length produces a lower overall reaction force, hence a smaller friction torque and work. Figure 4-4 displays the results of the variation in $\overline{\beta}$ and $\overline{W}$ for a range of $\overline{R}_{L3}$ from 1.0 to 7.0. In this figure the bearing radii are set equal to 1.0 or 0.5. For both bearing radii cases the work is minimized by a connecting rod length of approximately 1.8. To minimize the stress factors the connecting rod length increases to 3.0 to minimize $\overline{\beta}_1 = \overline{\beta}_2$, and to 5.5 when $\overline{\beta}_3$ is minimized. The estimated range of variations in the connecting rod length for the optimum mechanism is from 1.8 to 3.0 because once the length is increased past 3.0 both $\overline{W}$ and $\overline{\beta}_1 = \overline{\beta}_2$ increase. The actual range for the cases considered was from 2.25 to 3.12.

For all cases considered the radius of bearings 1 and 2 are smaller than that of bearing 3. This indicates that the maximum reaction forces for bearings 1 and 2 are smaller than that for bearing 3. Since the

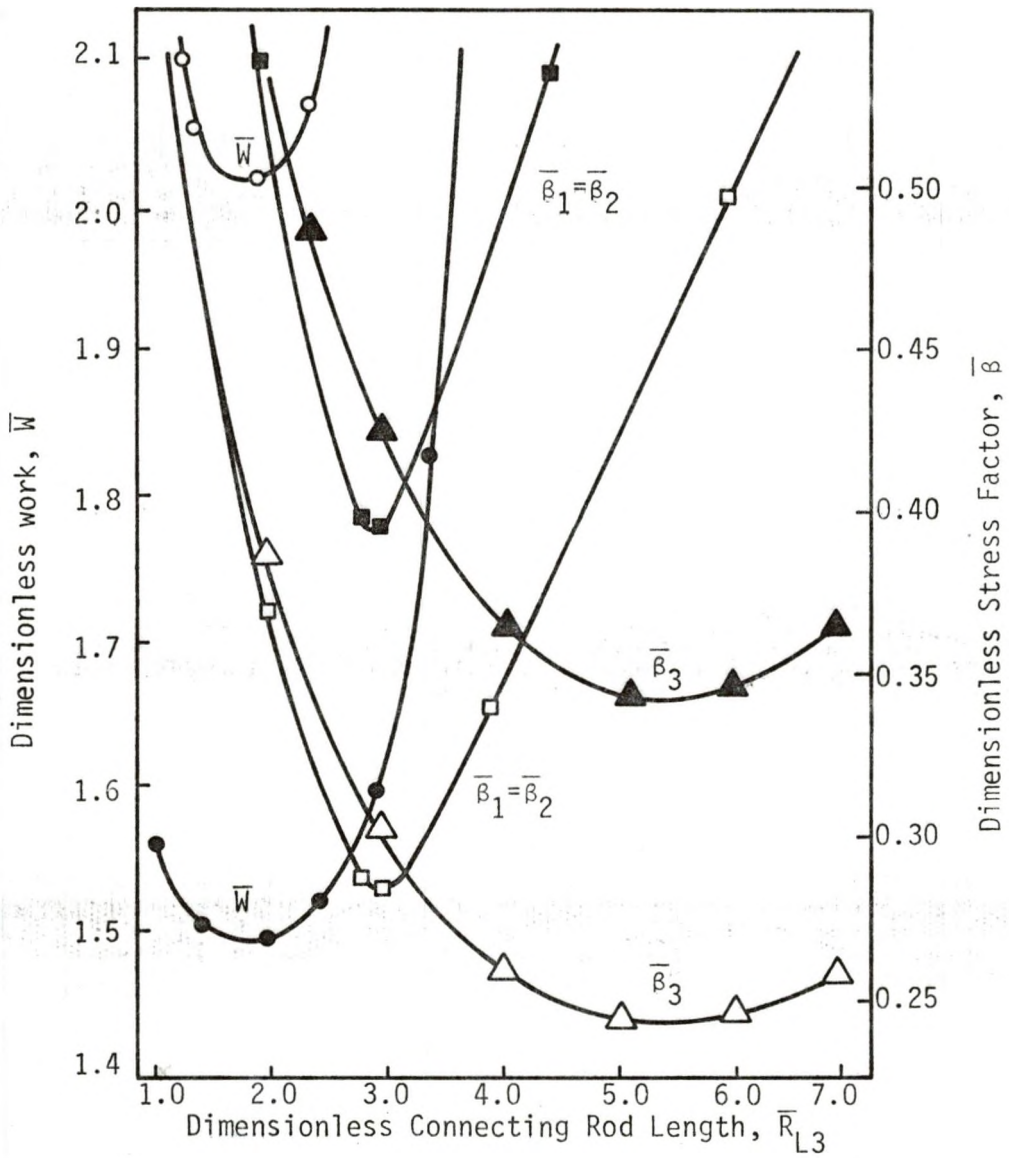

Legend:
△ = Stress Factor for Bearing 3
□ = Stress Factor for Bearings 1 and 2
○ = Work
△□○ = $\overline{R}_1 = \overline{R}_2 = \overline{R}_3 = 0.5$
▲■● = $\overline{R}_1 = \overline{R}_2 = \overline{R}_3 = 1.0$

These curves are plotted under the conditions:

$\mu = 0.1$, $\overline{H} = 0$, $\overline{R}_1 = \overline{R}_2 = \overline{R}_3$

FIGURE 4-4 - PLOT OF WORK AND THE STRESS FACTOR VERSUS CONNECTING ROD LENGTH WHEN THE BEARINGS ARE MASSLESS

maximum stress factors occur at approximately the same crank position, the inertia effects must tend to reduce the maximum reaction force. As suspected, as the weighting factor increases so do all the bearing radii. As the coefficient of friction increases the bearing radii decrease but the weighting factor required to obtain the same stress factor increases. This occurs since as the bearing radii or coefficient of friction increases so does the size of the friction circle and relative forces. It should be noted that when the sum of the friction circles for bearings 2 and 3 become approximately equal to the connecting rod length a situation occurs during the cycle for which no solutions exist, therefore the iterative technique used to determine the reaction forces diverges. None of the mechanisms listed exhibit this problem.

As shown in Figure 4-5, the work strictly increases with the bearing radii, since the increased bearing radii increase the friction torque. The stress factor decreases until the bearing radii increase to approximately 5.5 and 6; any further increases in the bearing radii increase the stress factors because the increase in the reaction forces, due to the increased friction torques for bearings 2 and 3, exceeded the increased area bearing the reaction force for large bearing radii.

4-4 Optimization Results That Consider All The Mechanism Mass

The majority of the bearing radii for the optimum mechanisms listed in Tables 4-3 and 4-4 are large. Since they become large, the massless model of the bearing is not an appropriate model. Therefore, a more appropriate model would include the inertia effects of the bearings. In this model, the journal-bearing has a journal that is a solid rod of radius R and an outer radius of the bearing surface equal to 1.5 R. The results for this model are presented in Tables 4-5 and 4-6, and Figure 4-6. These results

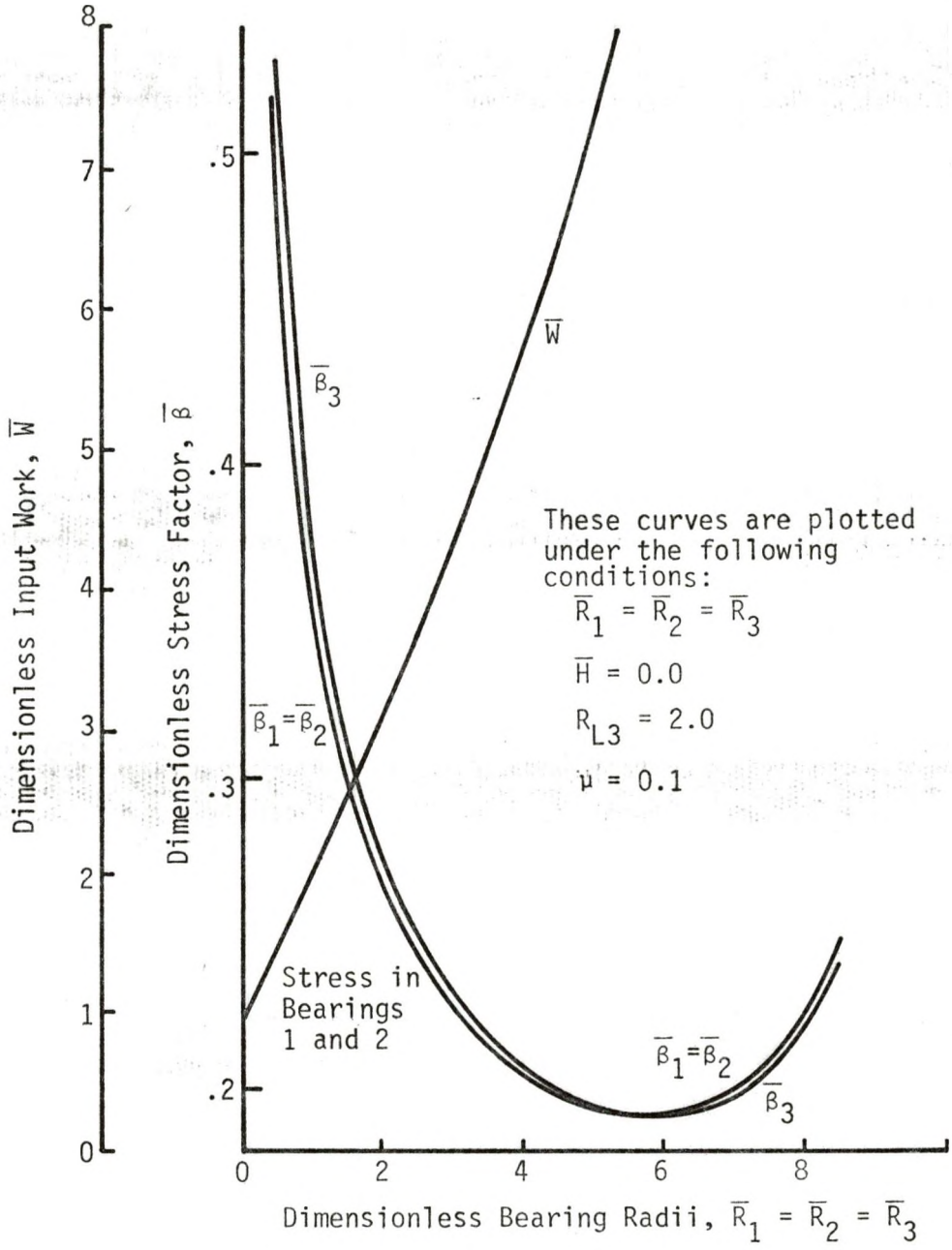

FIGURE 4-5 - PLOT OF WORK AND STRESS FACTOR VERSUS THE BEARING RADII WHEN THE BEARINGS ARE MASSLESS

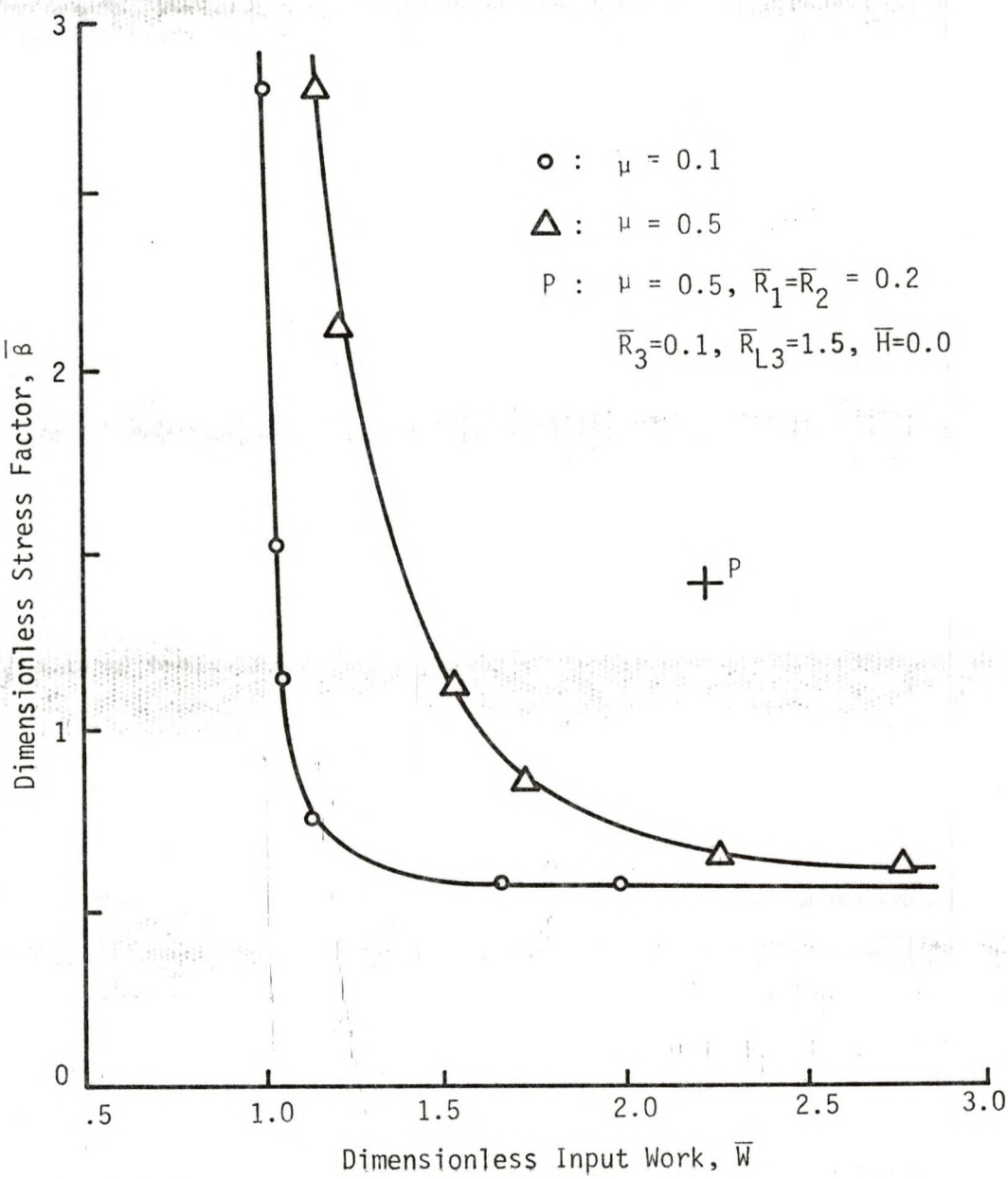

FIGURE 4-6 - FOR THE CASE OPTIMIZATION RESULTS CONSIDERING ALL MASSES

TABLE 4-5

OPTIMIZATION RESULTS FOR THE CASE WHEN ALL MASSES ARE CONSIDERED AND A COEFFICIENT OF FRICTION EQUAL TO 0.1

w	$\overline{W}$	$\overline{\beta}_1=\overline{\beta}_2$	$\theta^\circ(\overline{\beta}_1=\overline{\beta}_2)$	$\overline{\beta}_3$	$\theta^\circ(\overline{\beta}_3)$	$\overline{R}_{L3}$	$\overline{R}_1=\overline{R}_2$	$\overline{R}_3$
0.001	0.996	6.26	300	5.98	300	1.84	0.00362	0.00419
0.01	1.01	2.82	300	2.51	300	1.98	0.0161	0.0213
0.05	1.04	1.53	300	1.06	300	2.38	0.0417	0.100
0.1	1.06	1.17	300	0.921	300	2.58	0.0621	0.120
0.5	1.17	0.734	300	0.734	300	2.43	0.158	0.194
1.0	1.17	0.717	300	0.717	300	2.51	0.157	0.196
5.0	1.36	0.646	186	0.646	300	2.91	0.238	0.202
10.0	2.01	0.585	186	0.585	300	2.89	0.416	0.240
50	3.81	0.585	186	0.585	300	2.97	0.637	0.234

TABLE 4-6

OPTIMIZATION RESULTS FOR THE CASE WHEN ALL
MASSES ARE CONSIDERED AND A COEFFICIENT OF FRICTION EQUAL TO 0.5

w	$\overline{W}$	$\overline{\beta}_1=\overline{\beta}_2$	$\theta^\circ(\overline{\beta}_1=\overline{\beta}_2)$	$\overline{\beta}_3$	$\theta^\circ(\overline{\beta}_3)$	$\overline{R}_{L3}$	$\overline{R}_1=\overline{R}_2$	$\overline{R}_3$
0.001	1.18	12.8	300	12.8	300	1.70	0.000983	0.00102
0.01	1.20	5.00	300	4.99	300	1.85	0.00577	0.00608
0.05	1.25	2.86	300	2.86	300	2.01	0.0157	0.0170
0.1	1.30	2.16	300	1.83	300	2.12	0.0255	0.0386
0.5	1.56	1.17	294	1.17	300	2.86	0.0552	0.0681
1.0	1.69	0.934	294	0.934	300	2.87	0.0841	0.104
5.0	2.06	0.727	204	0.728	300	2.89	0.143	0.162
10	2.79	0.632	192	0.632	300	2.91	0.223	0.203
50	3.96	0.587	186	0.587	300	2.94	0.311	0.225

are for the inline slider-crank mechanism with a coefficient of friction equal to 0.1 and 0.5. As in the preceding cases, the tables contain data for the weighting factor, work, stress factor and crank position at which it occurs, and the mechanism dimensions.

The trade off curves of Figure 4-6 have a minimum obtainable stress factor equal to 0.56. Once the curves obtain a stress of 0.56, they terminate, any further increase in the dimensions to decrease the stress factor at the expense of the work would both increase the work and the stress factor. The trade off curves are also asymptotic to a line parallel to the stress axis when small values of w are considered. If there was no friction this line would have the equation $\overline{W} = 0.949$, which is the work required to complete a compression cycle. As w decreases, the friction effects at the journal bearings are negligible because the bearing radii become small and are zero when $w = 0$, but the friction effects at the slider still exist. For a coefficient of friction of 0.1 the minimum work is 0.993, or a 4.6 percent increase in work due solely to the friction effects between the slider and frame. The mechanism that generates this result has its bearing radii all equal to zero and a connecting rod length of 1.81. When the coefficient of friction is increased to 0.5 the minimum possible work is 1.18, a 24 percent increase over the frictionless case.

The addition of the bearing mass tended to produce a reduction in the bearing radii, and a slightly increased connecting rod length as compared to the massless bearing case. The reason for this change is that the area bearing the reaction force, for the bearings, is proportional to the connecting rod length and the bearing radius, therefore a decrease in bearing radius can be offset by an increase in the connecting rod length. This occurs because the bearing mass is directly related to the connecting rod

length and the bearing radius squared, so a trade off occurs between the area and mass.

Notice that the stress factors for the optimum mechanisms are approximately equal, therefore, adding to the justification for forcing the stress factors for bearings 1 and 2 to be equal. Also, as in previous cases, the mechanism dimensions increase when a reduction in stress is desired.

The general effect of variations in mechanism dimensions upon the work and stress factors are shown in Figures 4-7 and 4-8. Figure 4-7 shows that the work strictly increases with increasing bearing radii. This increase is due to the increased size of the friction circles and possibly due to the overall increase in the reaction forces produced by the added inertia effects produced by the increased bearing masses. The stress factors all reach a minimum and then increase as the bearing radii increase. The trade off in this instance is increased area bearing the reaction force versus the increased reaction forces due to the friction torque and possibly the inertia effects. In some instances, the inertia effects reduce the reaction forces but in other cases they increase the reaction forces. From Figure 4-8 the prediction that could be made is that the work strictly increases with increasing connecting rod length. This is not true for all cases; due to the large bearing radii used in this example the inertia effects predominate causing the work to increase. As stated earlier, the theoretical mechanism dimensions that minimize work are a finite connecting rod length, greater than zero, and bearing radii that are zero. The stress factors for bearings 1 and 2 reach a minimum and then increase again due to the increased inertia effects. The stress factor for bearing 3 levels off but does increase again once the inertia effects are large enough to become dominant.

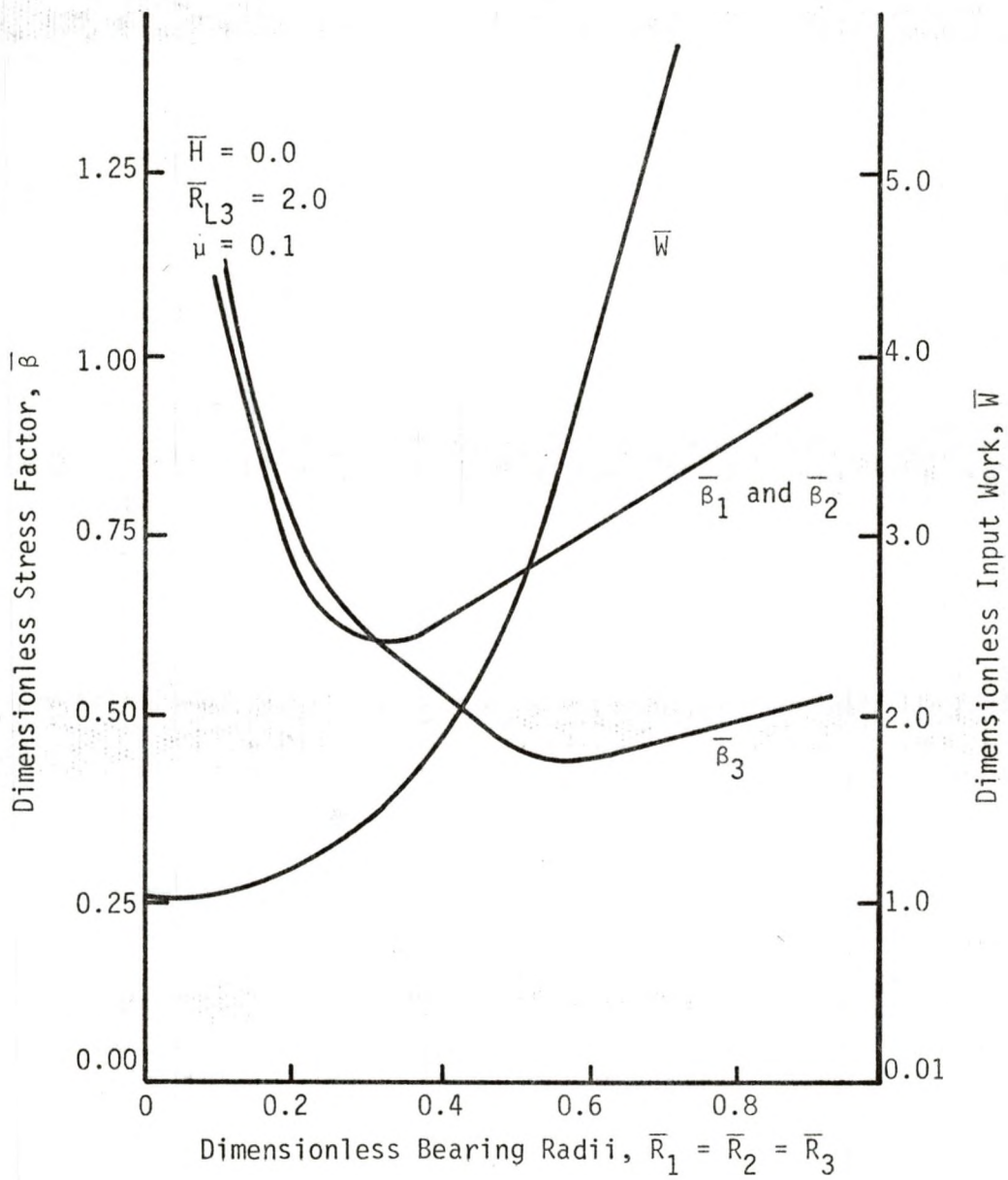

FIGURE 4-7 - PLOT OF WORK AND STRESS FACTORS VERSUS THE BEARING RADII

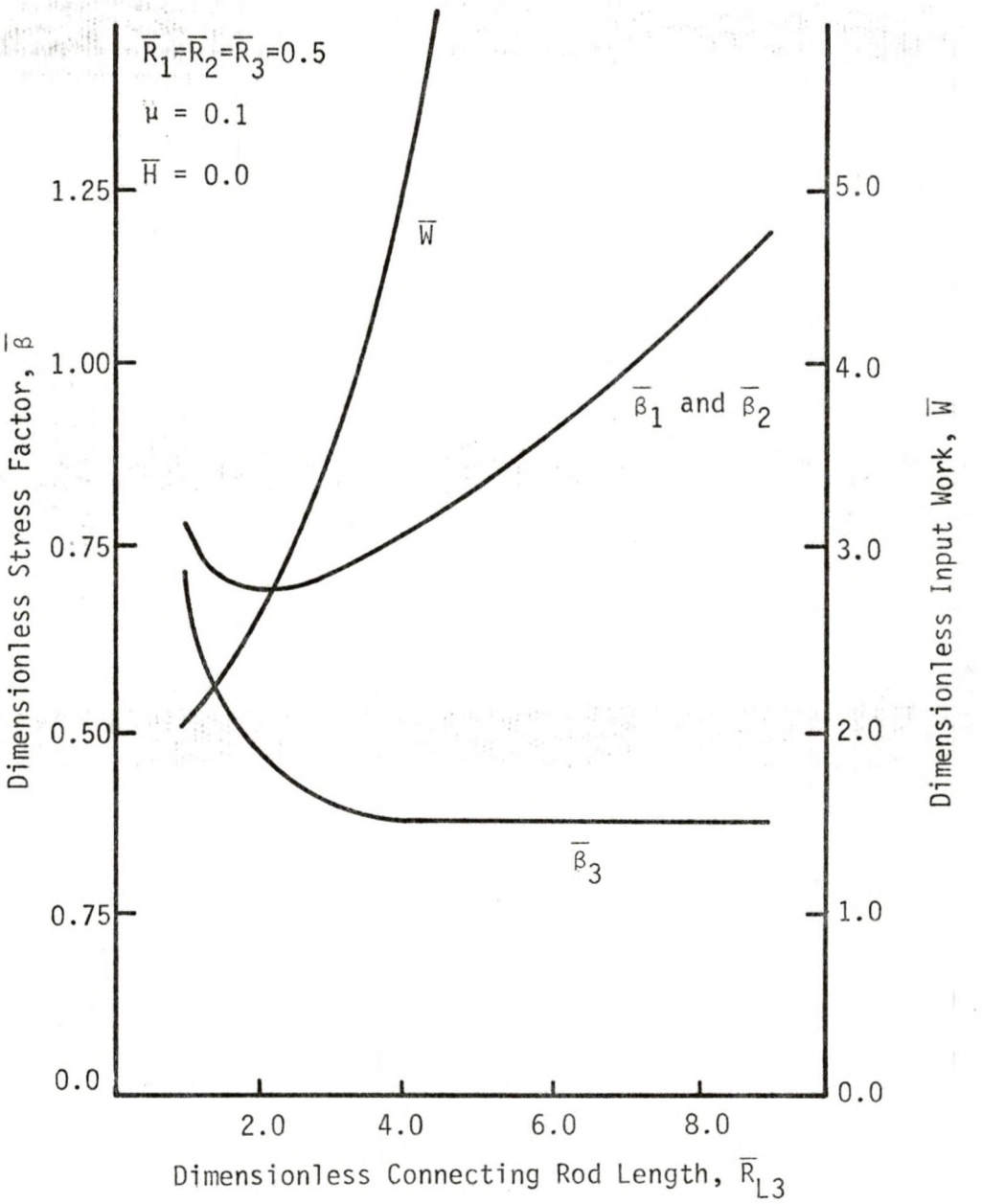

FIGURE 4-8 - PLOT OF WORK AND STRESS FACTORS VERSUS THE CONNECTING ROD LENGTH

Referring to Tables 4-5 and 4-6, it should be noted that the maximum stress factors for bearing 3 occur at 300°, which corresponds to the location where the maximum pressure occurs. The inertia effects do not become significant enough to change this location for bearing 3. The inertia effects do become dominant when the stress factors for bearings 1 and 2 are considered, as is shown by the change in the crank position for the maximum stress factor. The inertia effect dominates to such an extent that the bearing radii for bearings 1 and 2 become larger than bearing 3's radius. Therefore, the reaction forces due to inertia effects are greater than the forces produced by the maximum external load.

For the cases considered the trade off curves for Figure 4-6 most closely model an actual mechanism. The significance of these curves is illustrated when an arbitrary point P is considered. P represents an in-line slider-crank mechanism with the following dimensions:

$$\overline{R}_{L3} = 1.5$$

$$\overline{R}_1 = \overline{R}_2 = 0.2$$

$$\overline{R}_3 = 0.1$$

$$\mu = 0.5$$

For this mechanism the following work and stress factors exist: $\overline{W} = 2.22$, $\overline{\beta}_1 = \overline{\beta}_2 = 1.00$, $\overline{\beta} = \overline{\beta}_3 = 1.43$. This is a non-optimum mechanism that, for example, could be improved by using the optimum mechanism of Table 4-6 when $w = 1.0$. It can be seen that a 23 percent reduction in work and a 38 percent reduction in the maximum stress factor are obtainable by using an optimum mechanism.

4-5 Numerical Example

Suppose that an air compressor ($k = 1.4$) is to be designed for the following conditions:

displaced volume = 75.4 in^3

clearance volume = 7.54 in^3

cycle period = 0.105 sec

P_e = 60 psi

$P_i = P_a$ = 15 psi

The entire mechanism is to be constructed of steel with $E = 30\ (10^6)$ psi, $\mu_p = 0.3$ and $\rho = 0.28$ lbm/in^3. The piston has a mass of 5 lbm and a diameter of 4 inches. Assume that the coefficient of friction at all bearings is 0.5 and the clearance ratio $\alpha = 0.01$. Determine the optimum inline mechanism if the shear stress in the journal bearings is not to exceed 1250 psi.

From the above information, the basis for nondimensionalization is $S = 6$ inches, $M_4 = 5$ lbm, and $W_2 = 60$ rad/sec. The following nondimensional values of the various quantities are generated:

$\overline{P}_e = 7.65$

$\overline{P}_i = \overline{P}_a = 1.93$

$\overline{A}_p = 0.35$

$\overline{\rho} = 12.3$

$\alpha = 0.01$

$\overline{H} = 0$

$\overline{\tau}_{max} = 12.9$

$\overline{E} = 3.86\ (10)^6$

The dimensionless maximum allowable stress factor is calculated from equation (2-19) to be

$$\bar{\beta} = \frac{\bar{\tau}_{max}}{\sqrt{\frac{\bar{E}}{(1 - \mu_p^2)} \frac{\alpha}{(1 + \alpha)}}} = 0.791$$

Using this value of $\bar{\beta}$ and Table 4-6 the dimensionless optimum mechanism dimensions are determined by interpolating to be

$$\bar{R}_{L3} = 2.88$$

$$\bar{R}_1 = \bar{R}_2 = 0.125$$

$$\bar{R}_3 = 0.144$$

$$\bar{R}_{L2} = .5$$

The required dimensionless input work is also determined by interpolating to be 1.95. The dimensional form of these variables are

$$R_{L2} = 3"$$

$$R_{L3} = 17.3"$$

$$R_1 = R_2 = .75$$

$$R_3 = 0.864$$

The work required to drive this mechanism equals 273 ft-lb which corresponds to an input power requirement of 30 hp. The mechanism is shown in Figure 4-9.

4-6 Effect of Varying the Offset

Further reductions in the work and stress factor may be accomplished through the use of an offset slider-crank mechanism. When the offset is nonzero the mechanism exhibits quick return properties, that is, the time it takes the slider to move through a stroke in one direction differs from

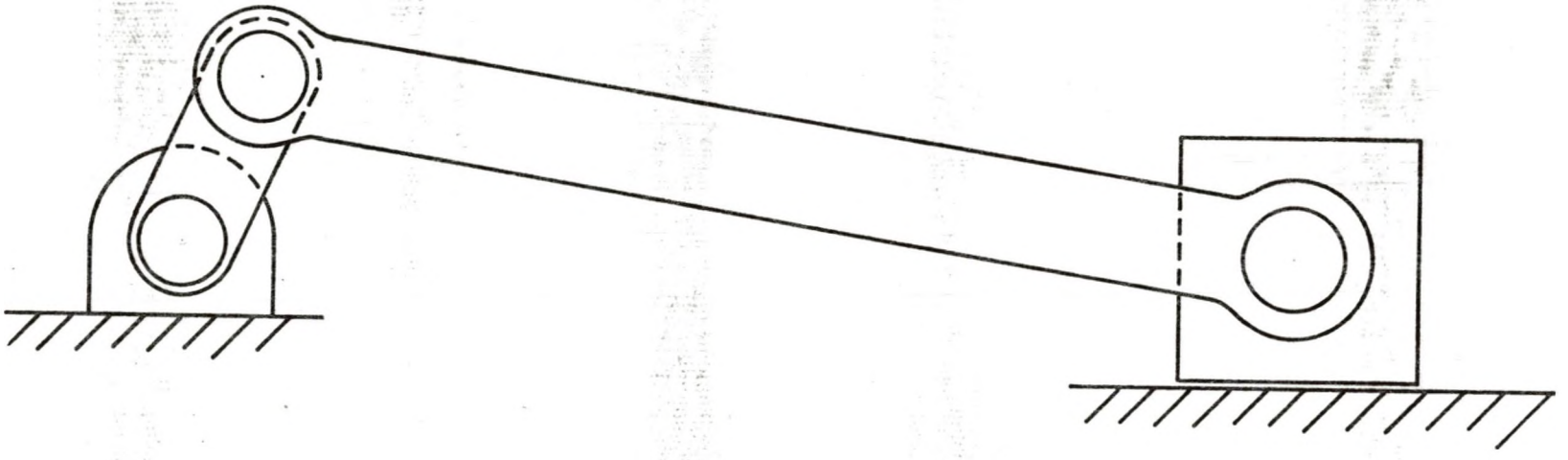

FIGURE 4-9 - OPTIMUM MECHANISM WHEN τ_{max} = 1250 PSI

the time to move through the stroke in the opposite direction. Since the time requirements differ and the distance of motion are the same, the velocities and accelerations are larger for the direction of motion which takes the smaller time. Then by properly adjusting the offset the inertia effects, the D'Alembert forces for the slider, may be varied so as to reduce the maximum reaction forces and thereby reduce the work and stress factor. Also, by the proper adjustment of the offset the connecting rod can be aligned with the direction of the external load when it is a maximum. Both of these adjustments require a negative offset.

To study the effects of the offset the optimization statement was modified to

$$\text{minimize } f = \overline{W} + w\overline{\beta} \qquad (4\text{-}5)$$

$$\text{with respect to } \overline{H}$$

This optimization statement was applied to the results for the inline slider-crank mechanism listed in Tables 4-5 and 4-6. The results of this optimization are listed in Table 4-7. In the table, both cases of coefficient of friction are considered (μ = .1 and .5) for various weighting factors. The results listed are the offset and the percent reduction in work and stress factor as compared to the inline mechanism.

It can be predicted from Figure 4-1 that the optimum offset should be negative. This prediction is supported by the results listed in Table 4-7. Also, it should be noted that all terms (i.e. $\overline{\beta}_1 = \overline{\beta}_2$, $\overline{\beta}_3$, and $\overline{W}$) do not obtain minimums for the same value of offset.

The general trends developed from the results are that larger simultaneous reductions in work and stress factors can be obtained for smaller weighting factors and larger coefficients of friction. Larger reductions are possible for the larger coefficients of friction because any reduction

TABLE 4-7

OPTIMIZATION RESULTS FOR THE OFFSET SLIDER-CRANK MECHANISM

	$\mu = .1$			$\mu = .5$		
w	$\overline{H}$	$\Delta\overline{W}$ %*	$\Delta\overline{\beta}$ %	$\overline{H}$	$\Delta\overline{W}$ %	$\Delta\overline{\beta}$ %
0.001	-0.4	1.2	1.8	-0.4	7.3	6.5
0.01	-0.5	1.1	1.9	-0.5	6.8	7.1
0.05	-0.5	0.6	1.4	-0.5	6.4	6.5
0.1	-0.5	0.8	1.3	-0.5	6.0	6.2
0.5	-0.2	0.0	0.3	-0.5	3.8	4.4
1.0	-0.3	-0.2	0.3	-0.4	2.6	3.6
5.0	-0.2	0	0.4	-0.1	0.6	1.0
10.0	-0.1	-0.1	0.1	-0.2	0.9	1.5
50.0	-0.1	0.05	0.1	-0.2	0.3	2.1

* A negative percent change in work represents an increase in the input work

in the reaction forces produce a reduction in the friction effects, so a larger coefficient of friction allows a larger reduction. For the larger weighting factor the inertia effects become dominant so the magnitude of the reduction in the reaction forces is reduced. The possible reduction by offsetting the slider range from approximately a seven percent reduction in work and stress factor to a 0.1 percent increase in work and 0.1 percent decrease in the stress factor.

In general, when the inertia effects are negligible substantial reduction in the objective function, f, can be obtained by varying the offset. As the inertia effects become significant, adjusting the offset produces smaller change in the objective function. When the inertia force becomes large, the change in the objective function with a properly adjusted offset is negligible.

CHAPTER 5

CONCLUSION

The procedure outlined in this thesis can be used to improve the input work and shear stress characteristics of slider-crank linkages. A single optimum mechanism does not exist, but a family of mechanisms do exist where each mechanism minimizes different levels of input work and shear stress. A more extensive family of tradeoff curves could be generated to cover a larger range of applied loads, coefficients of friction, and inertia effects.

5-1 Results

All of the trade off curves of the preceding chapter contained a transition from a line that is nearly vertical to a line that is nearly horizontal. The major difference in the mechanisms between these two extremes is the bearing size. When the curve is nearly a vertical line the bearing radii are small. Since the bearings are small, the friction torques are negligible as compared to the torque generated by the external load. Therefore, a small increase in these radii has a minimal effect upon the reaction forces and the input work. This increase will, however, produce a reduction in the shear stress proportional to $R^{-1/2}$. As the bearings become larger, the friction torques rival the torque produced by the external load for dominance, and the inertia forces increase. When this occurs a noticeable increase in the reaction forces occur. This increase is required to keep the mechanism in equilibrium. The increase in reaction forces increase the friction torques, and along with the increase in the moment arm this produces a nearly linear increase in work with

respect to bearing radii. Eventually, the bearings reach a limiting size where an increase in bearing radii no longer decreases the shear stress due to the increased reaction forces.

A relationship for the connecting rod is more difficult to determine because of the dependence upon this length by other parameters. In general, a shorter connecting rod is used when the optimization is weighted towards minimizing work instead of shear stress. As the shear stress becomes dominant in the optimization, a trade off occurs between the increased area bearing the reaction forces and the increased inertia effects, since the bearing length is proportional to the connecting rod length.

The final parameter is the offset. To optimize the mechanism the offset should be negative. This tends to align the connecting rod with the applied load, which reduces the reaction forces when the applied load is a maximum (compression-exhaust cycle). Also, the inertia effects are increased during the intake-expansion cycle which increase, and therefore the reaction forces when the applied load is a minimum. These effects produce a trade off used to determine the optimum offset.

5-2 Direction for Continued Research

An improvement in the optimization process is attainable if a technique is developed to determine exactly when the maximum shear stresses occur. If this were done, the optimization statement could include the bearing radii, connecting rod length, and offset simultaneously.

Another possibility for continuation of this work would be to analyze the stress generated in the connecting rod along with bearing shear stress and input work. By allowing different length to diameter ratios for the connecting rod the design parameters for the mechanism would include an acceptable maximum stress for the connecting rod. This would remove the

extra dependencies placed upon the connecting rod length. Another limitation could be the smallest acceptable journal bearing combination.

APPENDIX I

Computer Model of a Single Acting Compressor

```
* GENERAL COMMENTS ARE:1)COMMON/ALWAYS/ETC,CALL DFPM,SUBROUTINE
*GRADU ARE PARTS OF THE OPTIMIZATION PACKAGE.  THE VARIABLES NN,ACC,
*FC,FF,IGRAD,IOUT,KFEAS,LIM,METHOD,MINIM,NC,NI,NPERT,TMAX,AND TT ARE
*PARAMETERS IN THE OPTIMIZATION PACKAGE.  THE INTIAL GUESSES OF THE
*OPTIMUM ARE THE VALUES X(1),X(2),AND X(3).  WORK REFERS TO THE
*REQUIRED INPUT WORK.  STRS1,STRS2,AND STRS3 ARE THE MAXIMUM STRESS
*FACTORS FOR BEARINGS 1,2,AND 3.  THESE MAXIMUMS OCCUR WHEN THE CRANK
*ANGLE IS AN2 (STRS2 AND STRS1 ARE MAX) OR AN3 (STRS3 IS MAX).  THE
*TERM III IS A COUNTER USED TO COUNT THE NUMBER OF ITERATIONS NEEDED
*TO FIND THE OPTIMUM.  IF IOPT=1 A LISTING OF THE REACTION FORCES
*FOR A COMPLETE CRANK ROTATION WILL BE GENERATED.  THE LIST INCLUDES
*THE CRANK ANGLE,INPUT TORQUE,APPLIED LOAD,SLIDER PIN INERTIA FORCES,
*F34X,F23X,F34Y,F23Y,F34,F23,AND THE LAST TWO TERMS RELATE TO THE
*ACCURACY OF THE APPROXIMATIONS OF THE REACTION FORCES.
      COMMON/ALWAYS/TMAX,METHOD,KFEAS,LIM,NC,NI,IOUT,NPERT
      COMMON/OTPT/STRS1,STRS2,STRS3,WORK,WEIGHT,III,IOPT,AN2,AN3
      COMMON/OT/R1,R2,R3,RL3,H,RL2,U
      DIMENSION X(5)
1     FORMAT('1')
2     FORMAT('0','BEARING RADII:',3(1X,E13.6),'ANGLE',2(2X,F7.4))
3     FORMAT('0','    FORMAT',3(2X,E13.6))
4     FORMAT('0','WORK=',E13.6,' STRESSES=',3(1X,E13.6))
5     FORMAT('0','*****WEIGHT=',E11.4,'*****III=',I5,'*****U=',F6.3)
6     FORMAT('0','INTIAL X ARE:',5(2X,E11.4))
7     FORMAT('1',3X,'TH2',6X,'TORQUE',2X,'LOAD',6X,'IS',7X,'F34X',5X,
     $'F23X',5X,'F34Y',6X,'F23Y',6X,'F34',7X,'F',7X,'GG')
      U=.1
      NN=3
      ACC=.5E-06
      FC=10.
      FF=.01
      IGRAD=1
      IOUT=3
      KFEAS=1
      LIM=15
      METHOD=5
      MINIM=1
      NC=0
      NI=0
      NPERT=1
      TMAX=1.
      TT=.2
      IOPT=0
      X(1)=.001
      X(2)=.001
      X(3)=1.
      WRITE(6,6)(X(LLL),LLL=1,NN)
      CALL DFPM(MINIM,X,TT,NN,ACC,F,FF,IGRAD)
      CALL FUNCT(X,F)
```

```
      WRITE(6,4)WORK,STRS1,STRS2,STRS3
      WRITE(6,3)RL2,RL3,H
      WRITE(6,2)R1,R2,R3,AN3,AN2
      WRITE(6,5)WEIGHT,III,U
      IOPT=1
      WRITE(6,7)
      CALL FUNCT(X,F)
      CALL EXIT
      END
      SUBROUTINE GRADU(X,S,SUM)
      RETURN
      END
      SUBROUTINE FUNCT(XVAR,FUNC)
*THIS SUBROUTINE DETERMINES THE MASS,INERTIA,AND THE OBJECTIVE
*FUNCTION.  IT CALLS SUBROUTINES TO PERFORM THE KINEMATIC AND DYNAMIC
*FORCE ANALYSIS AND TO DETERMINE THE MAX REACTION FORCES.  THE
*TERMS USED ARE:CON-A CONSTANT USED TO DETERMINE THE MAX STRESS
*FACTOR,RR3-THE LENGTH OF THE CONNECTING BETWEEN THE BEARINGS,
*AM1,AM3-THE MASS OF THE BEARING PORTION OF THE CONNECTING ROD,
*AM2-THE MASS THE ROD PORTION OF THE CONNECTING ROD,AMT-THE TOTAL,
*MASS OF THE CONNECTING ROD,AMP3-THE MASS OF PIN3,AI#-THE MASS
*MOMENT OF INERTIA OF A PORTION OF THE CONNECTING ROD ABOUT IT'S
*CENTER OF MASS,AIT-THE TOTAL INERTIA OF THE CONNECTING ROD ,AND
*XCM- THE DISTANCE ALONG THE CONNECTING ROD FROM BEARING #2 TO
*THE CENTER OF MASS
      DIMENSION XVAR(5)
      COMMON/OTPT/STRS1,STRS2,STRS3,WORK,WEIGHT,III,IOPT,AN2,AN3
      COMMON/OT/R1,R2,R3,RL3,H,RL2,U
      COMMON/LOADR/CH1,CH2,XCH1,XCH2
      COMMON/FORIN/R32,AMT,AMP3,XCM,AIT,C1,FL
      COMMON/FOROUT/X,Y,Z,XX,YY,ZZ,B1,F,GG
      III=III+1
      R1=ABS(XVAR(1))
      R3=ABS(XVAR(2))
      RL3=XVAR(3)
      R2=R1
      H=0.
      PI=3.141592
      R32=RL3*RL3
      H2=H*H
      RL2=((4.*R32-1.-4.*H2)/(16.*R32-4.))**.5
      RHO=12.3
      CON=.1197/(1.+U*U)**.25
      RR3=RL3-1.5*(R2+R3)
      AM1=RHO*PI*RL3*R3*R3/8.
      AM2=RHO*PI*R32*RR3/400.
      AM3=RHO*PI*RL3*R2*R2/8.
      AMT=AM1+AM2+AM3
      AMP3=RHO*PI*RL3*R3*R3/10.
```

```
      XCM=((R2+RR3/2)*AM2+RL3*AM1)/AMT
      CONST=4./622.*RHO*PI*RL3
      AI1=CONST*R3**4+AM1*(RL3-XCM)**2
      AI2=AM2*(RR3*RR3+(RR3/2.+1.5*R1-XCM)**2)
      AI3=CONST*R2**4+AM3*XCM*XCM
      AIT=AI1+AI2+AI3
      C1=U/(U*U+1.)
*CH1,CH2,XCH1,XCH2 ARE USED WHEN THE APPLIED LOAD IS CALCULATED
      CH1=ARSIN(H/(RL3-RL2))+PI
      CH2=ARSIN(H/(RL3+RL2))
      XCH1=(RL3-RL2)*COS(CH1-PI)
      XCH2=(RL3+RL2)*COS(CH2)
      IF(CH2.LT.0.)CH2=CH2+2*PI
      TH2=0.
      FMAX1=0
      FMAX2=0
      Y=0.
      WORK=0.
      DANG=PI/30.
      DO 1 I=1,60
*SUBROUTINE FORCE PERFORMS THE KINEMATIC AND DYNAMIC FORCE ANALYSIS
      CALL FORCE(TH2,TORQUE)
      IF(FMAX1.LT.Z)AN3=TH2
      IF(FMAX1.LT.Z)FMAX1=Z
      IF(FMAX2.LT.ZZ)AN2=TH2
      IF(FMAX2.LT.ZZ)FMAX2=ZZ
      WORK=WORK+TORQUE
      IF(IOPT.EQ.0)GOTO 1
      WRITE(6,69)TH2,TORQUE,FL,B1,X,XX,Y,YY,Z,ZZ,F,GG
1     TH2=TH2+DANG
69    FORMAT('0',10(F8.3,1X),2(E9.1,1X))
*SUBROUTINE SEARCH DETERMINES THE MAX REACTION FORCES AND THEIR
*LOCATIONS
      CALL SEARCH(AN3,DANG,1,FMAX1)
      CALL SEARCH(AN2,DANG,2,FMAX2)
      STRS3=(FMAX1*10./R3/RL3)**.5*CON
      STRS2=(FMAX2*10./R2/RL3)**.5*CON
      STRS1=STRS2
      SS1=STRS3
      IF(STRS2.GT.SS1)SS1=STRS2
      FUNC=SS1*WEIGHT+WORK*DANG
      RETURN
      END
      SUBROUTINE FORCE(TH2,TORQUE)
      COMMON/OTPT/STRS1,STRS2,STRS3,WORK,WEIGHT,III,IOPT,AN2,AN3
      COMMON/OT/R1,R2,R3,RL3,H,RL2,U
      COMMON/LOADR/CH1,CH2,XCH1,XCH2
      COMMON/FORIN/R32,AMT,AMP3,XCM,AIT,C1,FL
      COMMON/FOROUT/X,Y,Z,XX,YY,ZZ,B1,F,GG
```

```
*THE KINEMATIC ANALYSIS
      X2=RL2*COS(TH2)
      Y2=RL2*SIN(TH2)
      X3=(R32-(H-Y2)**2)**.5
      TH3=ATAN((H-Y2)/X3)
      Y3=SIN(TH3)*RL3
      W3=-X2/X3
      W32=W3*W3
      AL3=Y2/X3+W32*Y3/X3
      AX=-X2-X3*W32-Y3*AL3
      VX=-Y2-W3*Y3
      XL=X2+X3
      S3=0.
      IF(S3.NE.0.)S3=-AB3(W3)/W3
      S4=0.
      IF(VX.NE.0.)S4=-ABS(VX)/VX
      AXCM=-X2-XCM*(AL3*SIN(PH3)+W32*COS(PH3))
      AYCM=-Y2+XCM*(AL3*COS(PH3)-W32*SIN(PH3))
*THE DYNAMIC FORCE ANALYSIS
      CALL LOAD(FL,XL,TH2)
      B1=(1.+AMP3)*AX
      B2=AMT*AXCM
      B3=AMT*AYCM
      B4=AIT*AL3
      B5=RL3-XCM
      B6=COS(PH3)
      B7=SIN(PH3)
      CC1=-C1*R1
      CC2=-C1*R2
      CC3=C1*R3*S3
      CC4=U*S4
      IF(I.LT.2)X=B1-FL
*THE ITERATIVE TECHNEQUE USED TO DETERMIN THE REACTION FORCES
      DO 10 IC=1,4
      XX=X-B2
      YY=Y-B3
      Z=(X*X+Y*Y)**.5
      ZZ=(XX*XX+YY*YY)**.5
      F=-B4-ZZ*CC2+Z*CC3+B6*(-B3*XCM-Y*RL3)+B7*(B2*XCM+X*RL3)
      GG=X+FL+ABS(Y)*CC4-B1
      GX=1
      GY=0
      IF(GY.NE.0)GY=CC4*ABS(Y)/Y
      FX=RL3*B7
      FY=-RL3*B6
      IF(ZZ.EQ.0.)GOTO 11
      FX=FX-XX*CC2/ZZ
      FY=FY-YY*CC2/ZZ
11    IF(Z.EQ.0.)GOTO 12
```

```
      FX=FX+CC3*X/Z
      FY=FY+CC3*Y/Z
12    D=GY*FX-FY*GX
      X=X+(FY*GG-GY*F)/D
10    Y=Y+(GX*F-GG*FX)/D
      XX=X-B2
      YY=Y-B3
      ZZ=(XX*XX+YY*YY)**.5
      TORQUE=YY*X2-XX*Y2-ZZ*(CC1+CC2)
      RETURN
      END
      SUBROUTINE LOAD(FL,XX,TH2)
*THIS SUBROUTINE CALCULATES THE APPLIED LOAD
      COMMON/LOADR/CH1,CH2,XCH1,XCH2
      A=.35
      PAT=1.932*A
      PE=7.6462*A
      PI=PAT
      PR=(PE/PI)**(1./1.4)
      XL=(XX-XCH2)/(XCH1-XCH2)
      XCH=1.1/PR-.1
      XCHECK=.1*PR-.1
      IF(CH2.GT.3.)GOTO 8
      IF(TH2.LT.CH1.AND.TH2.GT.CH2)GOTO 1
      GOTO 9
8     IF(TH2.LT.CH1.OR.TH2.GT.CH2)GOTO 1
9     FL=PAT-PI*(1.1/(XL+.1))**1.4
      IF(XL.GT.XCH)FL=PAT-PE
      RETURN
1     FL=PAT-PE*(.1/(XL+.1))**1.4
      IF(XL.GT.XCHECK)FL=PAT-PI
      RETURN
      END
      SUBROUTINE SEARCH(ANG,DANG,MCH,FMAX)
*THIS SUBROUTINE PROVIDES A SEARCH TO DETERMINE THE LOCATION
*AND MAGNITUDE OF THE MAXIMUM REACTION FORCES.  IF MCH IS 2
*THE MAX FORCE FOR BEARINGS 1 AND 2 IS DETERMINED,ALL
*OTHER VALUES DETERMINE THE MAX FORCE FOR BEARING 3.
      COMMON/OTPT/STRS1,STRS2,STRS3,WORK,WEIGHT,III,IOPT,AN2,AN3
      COMMON/OT/R1,R2,R3,RL3,H,RL2,U
      COMMON/LOADR/CH1,CH2,XCH1,XCH2
      COMMON/FORIN/R32,AMT,AMP3,XCM,AIT,C1,FL
      COMMON/FOROUT/X,Y,Z,XX,YY,ZZ,B1,F,GG
      DIMENSION XS(3),YS(3)
      XS(2)=ANG
      YS(2)=FMAX
      DA=DANG/2.
      YS(1)=0
      YS(3)=0.
```

```
      DO 3 IN=1,7
      IF(YS(1).LT.YS(2))GOTO 1
      XS(2)=XS(1)
      XS(3)=XS(1)+DA
      XS(1)=XS(1)-DA
      YS(2)=YS(1)
      GOTO 4
1     IF(YS(3).LT.YS(2))GOTO 2
      XS(2)=XS(3)
      XS(1)=XS(3)-DA
      XS(3)=XS(3)+DA
      YS(2)=YS(3)
      GOTO 4
2     XS(1)=XS(2)-DA
      XS(3)=XS(2)+DA
4     DO 5 N=1,3,2
      A=XS(N)
      CALL FORCE(A)
      YS(N)=Z
5     IF(MCH.EQ.2) YS(N)=ZZ
3     DA=DA/2.
      FMAX=YS(2)
      RETURN
      END
```

REFERENCES

1. Baumeister, T., Mark's Standard Handbook For Mechanical Engineers, 7th Edition, McGraw Hill, New York, New York, 1967, pp. 3-34-37.

2. Sadler, J.P., and Mayne, R.W., "Balancing of Mechanisms by Non-linear Programming," Proceedings of the 3rd Applied Mechanism Conference, Oklahoma State University, November 1973, pp. 29.1-29.17.

3. Lee, T.W., "Optimization of High Speed Geneva Mechanisms," Journal of Machine Design, Vol. 103, No. 3, July 1981, pp. 621-30.

4. Root, R.R., and Ragsdell, K.M., "A Survey of Optimization Methods," ASME, Design Engineering Division, Paper No. D5-DET-95, 1975.

5. Yang, A.T., Pennock, G.R., and Hisa, L.M., "Stress Fluctuations in High Speed Mechanisms," Journal of Machine Design, Vol. 104, No. 4, October 1981, pp. 736-42.

6. Kubo, A., Okamoto, T., and Kurokawa, N., "Contact Stress Between Rollers with Surface Irregularity," Journal of Machine Design, Vol. 103, No. 2, April 1981, pp. 492-98.

7. Rohn, D.A., Loewenthal, S.H., and Coy, J.J., "Simplified Fatigue Life Analysis for Traction Drive Contacts," Journal of Machine Design, Vol. 103, No. 2, April 1981, pp. 430-39.

8. Spotts, M.F., Design of Machine Elements, 5th Edition, Prentice Hall, Englewood Cliffs, New Jersey, 1978, pp. 389-90.

9. Rooney, G.T., and Deravi, P., "Coulomb Friction and Mechanism Sliding Joints," Mechanism and Machine Theory, Vol. 17, No. 3, 1982, pp. 207-11.

10. Iman, I., Skreiner, M., and Sadler, J.P., "A New Solution to Coulomb Friction in Mechanism Bearings: Theory and Application," Journal of Mechanical Design, Vol. 103, No. 4, October 1981, pp. 764-75.

11. Shigley, J.E., Mechanical Engineering Design, McGraw Hill, New York, New York, 1977, pp. 74-78.

12. Van Wylen, G.J., and Sonntag, R.E., Fundamentals of Classical Thermodynamics, 2nd Edition, Wiley, New York, New York, 1973, pp. 226-32.

13. Roberson, J.A., and Crowe, C.T., Engineering Fluid Mechanics, Houghton Mifflin, Boston, Massachusetts, 1973, pp. 215-27.

14. Afimiwala, K.A., and Mayne, R.W., "Program Package for Design Optimization," State University of New York at Buffalo, 1974.

15. Fox, R.L., Optimization Methods for Engineering Design, Addison-Wesley, Reading, Massachusetts, 1971, pp. 104-10.

16. Martin, G.H., Kinematics and Dynamics of Machines, Revised Printing, McGraw Hill, New York, New York, 1969, pp. 357-83.